Chapter- 4

Isolation & identification of effective phytocomponents from active extracts of *Bauhinia variegata* L. by analytical methods and to examine its effects on cytotoxic parameters in lung cancer cell lines.

4.1 Introduction

The plant-based secondary metabolites are highly promising and advantageous in the field of medicine and are taxonomically distinct. The Indian Ayurveda method, which is primarily derived from plants, has been demonstrated to be largely effective in treating a wide range of illnesses. Plant extracts have been used to treat asthma, ulcers, sleeplessness, dementia, and bronchitis, among other conditions[1,2,3]. Plant phytochemicals can be produced from any part of the plant, including the bark, leaves, flowers, roots, fruits, seeds, etc., in conjunction with secondary metabolites that are unique to each type of plant[4,5,6].

Individual chemical compounds are separated from mixtures of chemical compounds using various chromatographic techniques[7]. *Bauhinia variegata* petroleum ether bark extracts and Chloroform bark extracts were extracted with standardised solvent systems and conventional methodology. Chromatographic techniques like TLC, HPLC and GC-MS was used for the separation of phytocomponents[8,9,10] and studied for their anti-cancer and apoptotic assays using A549 and H460 cell lines.

There are two sections in this chapter:

Section I - Isolation of phytocomponents from active extracts (PEBE & CBE) of *Bauhinia variegata* L. by analytical methods.

Section II – To study the cytotoxic effects of PEBE and CBE phytocomponents against lung cancer cell lines and identification of effective phytocomponents by analytical methods.

Section I - Isolation of phytocomponents from active extracts (PEBE & CBE) of *Bauhinia variegata* L. by analytical methods.

4.2 Materials and methods

4.2.1 Chemicals

The solvents used for extraction of phytocomponents from PEBE and CBE were of A.R. grade and was procured from Himedia Laboratories Pvt. Silica (60-200) mesh were obtained from SRL. Silica gel 60G F_{254} (DC Kiselgel 60 F_{254}) pre-coated thin layer chromatography plates were obtained from Merck, India. Infrared spectroscopy was noted on a FT-IR spectrophotometer Shimadzu 8201 PC (4000–400 cm^{-1}). Dimethyl sulphoxide-d6 for NMR

spectroscopy was purchased from SRL. Oleic acid and Palmitic acid was purchased from Himedia Laboratories Pvt, Heptadecanoic acid was purchased from Sigma- Aldrich. Bovine Serum albumin fatty acid free from Sigma- Aldrich, Sterile cell culture treated flasks, plates were obtained from NEST and Corning Inc. Sterile tubes from Tarsons. Dulbecco's modified eagle medium (DMEM) High Glucose, from Himedia Pvt Ltd, 3-(4,5-dimethylthiazol-2-yl)-2,5-diphenyltetrazolium bromide (MTT), Fetal Bovine Serum-U.S. origin from Himedia and Hyclone (Cytiva), Trypsin- EDTA (1x-0.25%)solution from Himedia, Penicillin-Streptomycin-Neomycin (PSN) Antibiotic mixture Thermo Fischer Scientific, PBS (Himedia) and also prepared in the laboratory with the standard protocol.

4.2.2 Preliminary phytochemical screening

The preliminary phytochemical analysis of crude extracts[9] of *Bauhinia variegata* was done to determine the presence of different phytochemicals in them (as described in Chapter 3).

4.2.3 Optimization of TLC solvent system for column chromatography

The components from effective extracts, Petroleum ether bark extract (PEBE) and Chloroform bark extracts (CBE) (as explained in Chapter 3) were separated by column chromatography using defined solvent systems. Different solvent systems were run for optimization of TLC system for PEBE and CBE of *Bauhinia variegata*. Silica layered on aluminum plates were used for the runs (Merck TLC Silica gel 60 F254). On the basis of literature study[8,9,10,], TLC was tried out with combinations of non-polar solvents. 0.5mg and 1mg amount of PEBE and CBE was spotted onto the silica plate in each case. Spots were imaged under UV at 254nm, 365nm and by staining with iodine vapors. The plates come with a UV active dye that shows green fluorescence at 254nm, enabling easy visualization of the compound.

4.2.3.1 Isolation and partial Characterization of Phytocomponents from PEBE and CBE of *Bauhinia variegata* by Column chromatography

Principle: The technique is based on differential adsorption of the extract to the stationary phase and the mobile phase. The interplay between the adsorption of the molecules to the stationary phase and the solubility of the molecule in the solvent mobile phase determines how long the molecules are retained in the column – retention time. Depending on their properties, different molecules have different retention times allowing for their separation.

4.2.3.2 Protocol for Column Chromatography – For PEBE

The column was packed with 30gm of silica gel (60-200 mesh) by wet filling method and then it had been crowded with eluting solvent of the lowest polarity i.e., Petroleum ether., in the column having G1 sintered glass disc (as shown in Figure 4.1). The silica gel (stationary phase) was poured into the column to form a bed of silica. The silica was allowed to settle and left still for an hour. Care was taken not to introduce any air bubble[10,11]. 2.3 gm PEBE (finely grated) was mixed with silica gel until a homogenous powder was form, covered with sand and then poured on to the bed of silica in the column. The column was allowed to run slightly till the PEBE completely adsorbed to the silica. The column was charged for 1hr for complete saturation with no bubble to make the bed static. Solvent level was made up and stopcock was opened to collect eluent (each of 3-5ml) with a step gradient solvent system from low to high polarity ie., PE-(100:0), PE:BZ= (90:10, 80:20, 70:30, 60:40, 50:50)BZ-(100:0), BZ:EA-90:10, 80:20, 70:30, 60:40, 50:50), EA-(100:0). 91 fractions were collected and subordinated to TLC with defined solvent system. The fractions were collected at uniform rate under gravity, dried and concentrated. For the purpose of identifying the appropriate bands, TLC was applied to all of the concentrated fractions. The fractions were stored at 4°C in sterile glass brown bottles for the further studies.

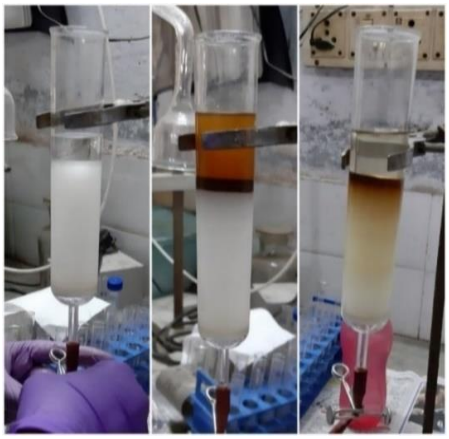

Column specifications: -

Column Dimension: 15 cm in length, 5.5 cm in diameter

Stationary phase – Silica gel G (60-120 mesh)

Mobile phase – Petroleum ether, Benzene & Ethyl acetate

Charged material – Petroleum ether extract of *Bauhinia variegata*

Figure 4.1 Setup for column chromatography

4.2.3.3 Thin Layer Chromatography (TLC)

TLC helps in partial separation of phytocomponents using silica coated TLC chromatographic plates. All the fractions were applied on activated TLC plates and plate is kept under standardized solvent system in a developing chamber [8]. Plates were taken out of the developing chamber; dried and solvent front was marked on the plate by pencil. Spots were visualized on

TLC plates under UV light (254nm). The visualized spots were marked on TLC plates and Rf value of each spot is calculated as

Rf = Distance travelled by the sample (cm)

Distance travelled by the solvent (cm)

TLC plates showing number of bands can be identified using high performance liquid chromatography (HPLC), Infrared (IR), Gas Chromatography and Mass spectrometry (GC/MS) and Nuclear magnetic resonance (NMR).

4.2.3.4 Protocol for Column Chromatography - Protocol for CBE

For CBE, the column was packed with 30gm of silica gel (60-200 mesh) by wet filling method and then it had been crowded with eluting solvent of the lowest polarity i.e., Chloroform, in the column having G1 sintered glass disc (as shown in Figure 4.2). The silica gel (stationary phase) was poured into the column to form a bed of silica. The silica was allowed to settle and left still for an hour[8,9,10,11]. 3.3 gm CBE (finely grated) was mixed with silica gel until a homogenous powder was form, covered with sand and then poured on to the bed of silica in the column. The column was allowed to run slightly till the CBE completely adsorbed to the silica. The column was charged for 1hr for complete saturation with no bubble to make the bed static. Solvent level was made up and stopcock was opened to collect eluent (each of 3-5ml) with a step gradient solvent system from low to high polarity ie., CHL-(100:0), CHL:EA=(90:10, 80:20, 70:30, 60:40,50:50), EA-(100:0), EA:MET-(90:10, 80:20, 70:30, 60:40,50:50), MET:EA (10:90), MET-(100:0). 73 fractions were collected and subordinated to TLC as explained above in 4.2.3.3.

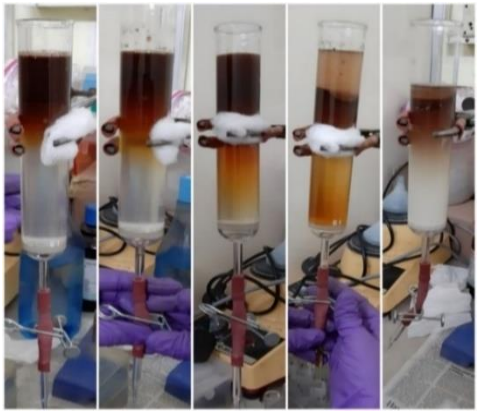

Column specifications:

Column Dimension: 15 cm in length

5.5 cm in diameter

Stationary phase – Silica gel G (60-120 mesh)

Mobile phase – Chloroform, Ethyl acetate & Methanol

Charged material – Chloroform extract of *Bauhinia variegata*

Figure 4.2 Setup for column chromatography (CBE)

4.3 Results and Discussion

4.3.1 Standardization of solvent system for PEBE and CBE

Different combination of solvents at various ratios were run and the best separation was observed in Petroleum Ether: Benzene: Ethyl Acetate – 8:1:1 for PEBE (as shown in Figure 4.3) and Chloroform: Ethyl acetate: Methanol (7:2:1) for CBE (as shown in Figure 4.4).

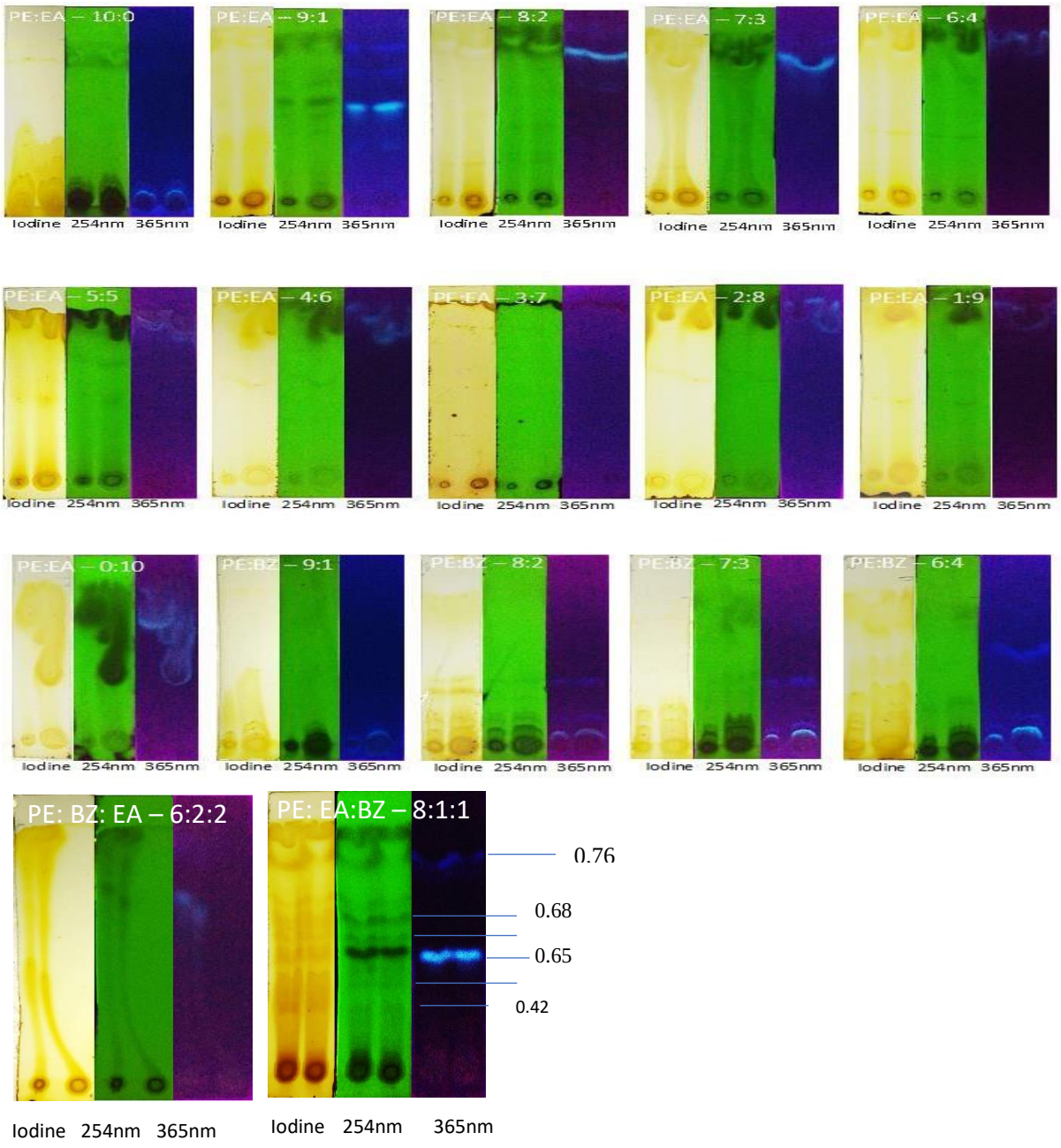

Figure 4.3 TLC profiles of different combinations of PE: BZ: EA.

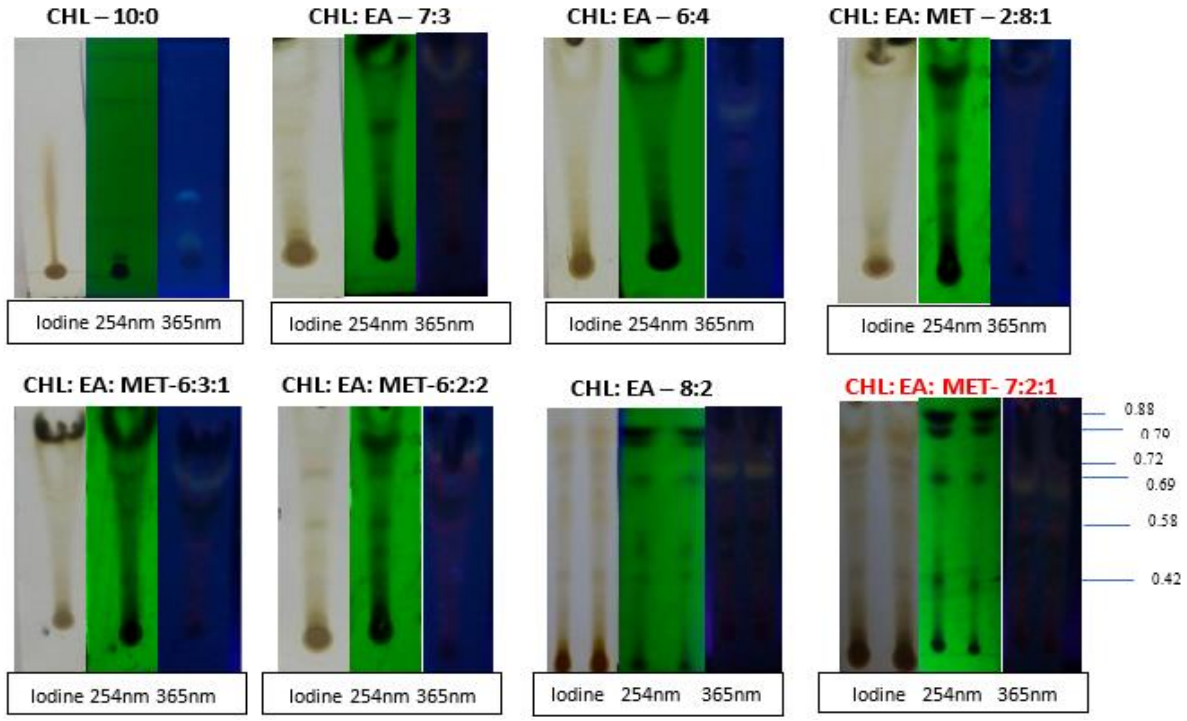

Figure 4.4 TLC profiles of different combinations of CHL: EA: BZ.

4.3.1.1 Fractionation and Identification of Fractions by Thin Layer Chromatography (PEBE)

The fractions obtained from column chromatography of *Bauhinia variegata* PEBE were further subjected using TLC. The phytocompounds showing the same Rf values were pooled into a single fraction. The total number of active fractions obtained after pooling were as follows: The elutes 29-36 aliquots of 20 ml each in solvent systems PE:BZ (60:40) formed Fraction P1, 37-47 aliquots PE:BZ (50:50) formed Fraction P2; the elutes 48-54 aliquots in solvent systems BZ (100:0) formed Fraction P3, the elutes 55-59 in solvent systems BZ:EA (90:10) formed Fraction P4, the elutes 60-66 in solvent systems BZ:EA (80:20) formed Fraction P5, the elutes 67-73 in solvent system BZ:EA (70:30) formed Fraction P6, the elutes 74-79 in solvent system BZ:EA (60:40) formed Fraction P7, the elutes 80-85 in solvent system BZ:EA (50:50) formed Fraction P8. The yields of the fractions obtained are shown in Table 1.

Table 4.1: Fractionation of Petroleum ether extract of *Bauhinia variegata* by column chromatography

Fraction no.	Mobile phase and Ratio(%)	TLCspots & Rf value	Compound (s) isolated	% Yield (w/w)
1-2	PE (100:0)	-	-	-

3-10	PE:BZ (90:10)	-	-	-
11-18	PE:BZ(80:20)	-	-	-
19-28	PE:BZ(70:30)	-	-	-
29-36	PE:BZ(60:40)	1 (0.91)	P1	0.05
37-47	PE:BZ (50:50)	1 (0.97)	P2	0.03
48-54	BZ(100:0)	2 (0.75,0.42)	P3	0.09
55-59	BZ:EA(90:10)	2 (0.97,0.85)	P4	0.37
60-66	BZ:EA(80:20)	2 (0.84,0.95)	P5	0.68
67-73	BZ:EA(70:30)	2 (0.85, 0.74)	P6	0.59
74-79	BZ:EA(60:40)	3 (**0.57**,0.82, 0.97)	P7	0.37
80-85	BZ:EA(50:50)	2 (0.71,**0.61**)	P8	0.02
86-91	EA(100:0)	1 (0.92)	P9	0.05

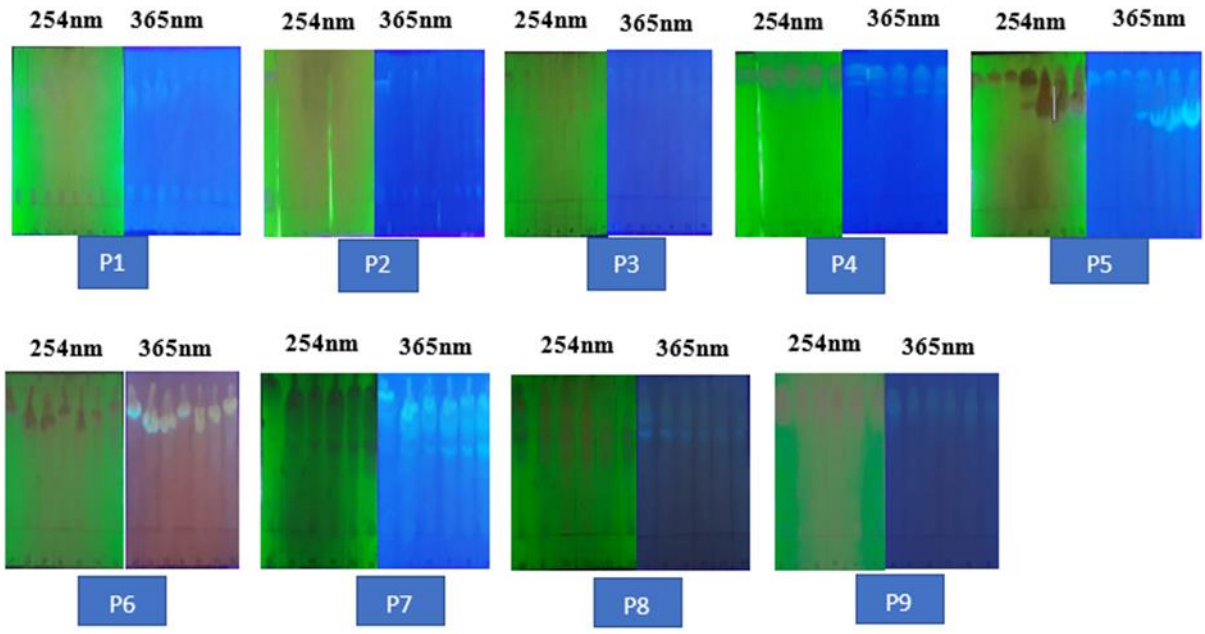

Figure 4.5 Identification of clear spots of PEBE fractions under UV 254 nm and 365 nm.

4.3.1.2 Fractionation and Identification of Fractions by Thin Layer Chromatography (CBE)

The fractions obtained from column chromatography of CBE of *Bauhinia variegata* further separated using TLC. The selection of solvents in an organized order shows the effect of polarity on the extraction and the extracted phytochemicals. The phytocompounds showing the

same Rf values were pooled into a single fraction. The total number of active fractions obtained after pooling were as follows: The elutes 12-18 aliquots of 20 ml each in solvent systems CHL:EA (70:30) formed Fraction F1, 19-26 aliquots CHL:EA (60:40) formed Fraction F2; the elutes 27-33 aliquots in solvent systems CHL:EA(50:50) formed Fraction F3, the elutes 34-39 in solvent systems EA (100%) formed Fraction F4, the elutes 40-45 in solvent systems EA:MET (90:10) formed Fraction F5, the elutes 46-52 in solvent system EA:MET (80:20) formed Fraction F6, the elutes 53-58 in solvent system EA:MET (70:30) formed Fraction F7, the elutes 59-63 in solvent system EA:MET (60:40) formed Fraction F8 as shown in Table 2.

Table 4.2: Fractionation of Chloroform bark extract of *Bauhinia variegata* by Column Chromatography

Fraction no.	Mobile phase and Ratio(%)	TLCspots & Rf value	Compound (s) isolated	% Yield (w/w)
1-3	CHL (100:0)	-	-	-
4-7	CHL: EA (90:10	-	-	-
8-11	CHL: EA (80:20)	-	-	-
12-18	CHL: EA (70:30)	2 (0.88,0.79)	F1	0.26
19-26	CHL: EA (60:40)	3 (0.91,0.84,0.74)	F2	0.40
27-33	CHL: EA (50:50)	2 (0.84,0.82)	F3	0.58
34-39	EA (100%)	1 (0.92)	F4	0.42
40-45	EA: MET (90:10)	1 (0.94)	F5	0.36
46-52	EA: MET (80:20)	1 (0.94,0.69)	F6	0.31
53-58	EA: MET (70:30)	2 (0.88,0.83)	F7	0.21
59-63	EA: MET (60:40)	1(0.88)	F8	0.13
64-70	EA: MET (50:50)	-	F9	-
70-73	MET (100%)	-	F10	-

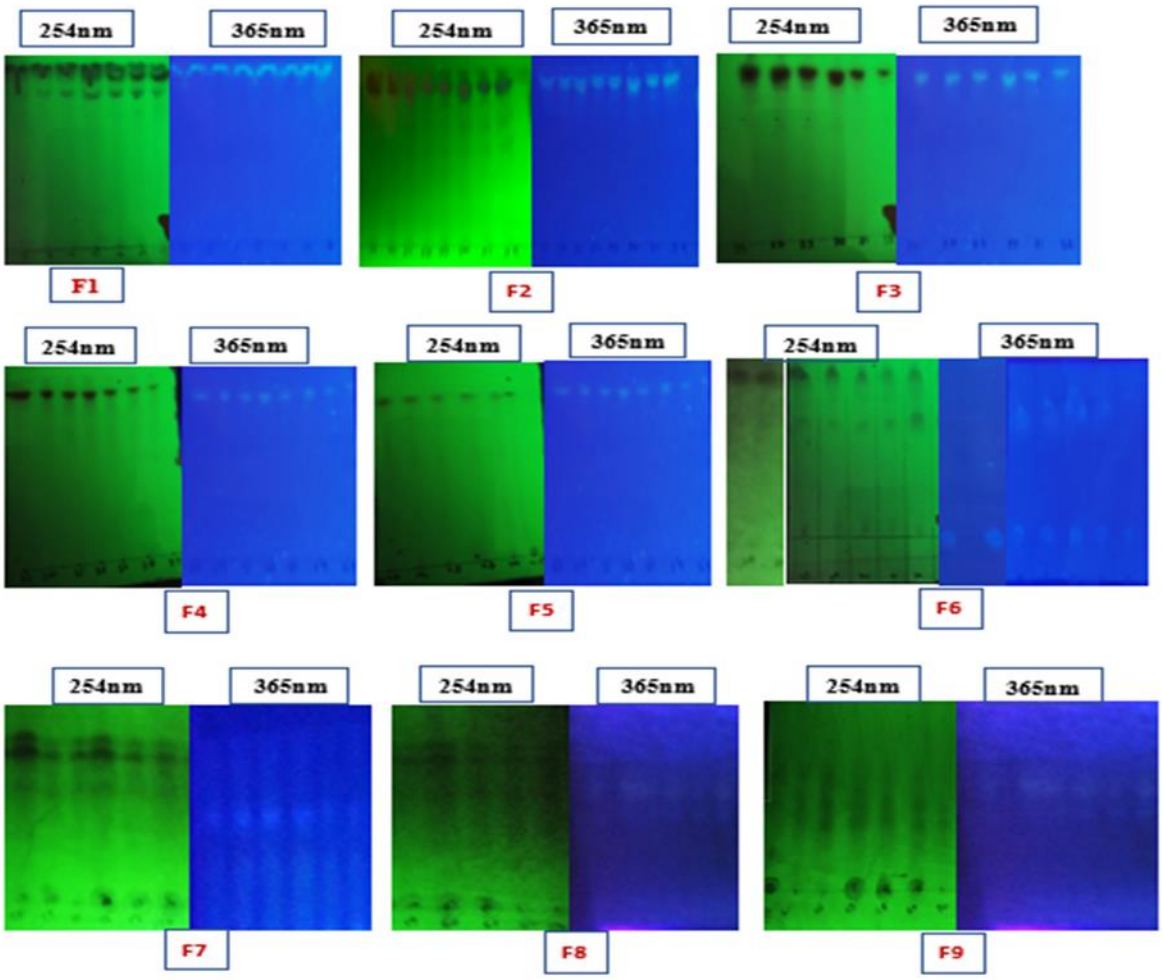

Figure 4.6 Identification of clear spots fractions under UV 254 nm and 365 nm.

Section II a) - To study the cytotoxic effects of PEBE and CBE phytocomponent/s against lung cancer cell lines and identification of effective phytocomponents by analytical methods.

4.4 Material and methods

4.4.1 Identification, characterization and cytotoxic effect of the effective phytocomponents of PEBE on A549 cell line.

4.4.1.1 To check the effect of active pytocomponents from PEBE on A549 cell line by MTT assay

The cytotoxic effect of all the isolated fractions from PEBE was checked on A549 cell line by MTT assay (as described in section 3.5.1.1).

4.4.1.1.1 Conjugation of Fatty acid to Bovine Serum Albumin(BSA) and its use for MTT assay

Rationale

Long chain free fatty acids (FFA) are typically delivered predominantly through creating hydro soluble lipoproteins with proteins in the blood. However, serum albumin, a protein that is prevalent in plasma and interstitial fluids and can bind fatty acids (FA)

and other lipophilic molecules, is the primary carrier of non-esterified FAs. Interactions between albumin and FA increase the quantity of Fatty acids delivered and remove it from the bloodstream. However, one of the main drawbacks for *in vitro* research is the limited solubility of long-chain Free FAs in aqueous solutions. FFAs can be conjugated to bovine serum albumin, which is analogous to the transport of long chain FFA in the blood to cells, to solve this issue. Saponification doesn't yield harmful solvent effects as sodium salts of FFA are formed by usage of NaOH or NaCl. As the molecules identified were FA, they had to be conjugated to BSA for use as anticancer agents.

- **Protocols for free fatty acid preparation and conjugation (OA/PA)**

1) Prepare 150mM NaCl sol.

2) Preparing BSA Solution:

- Prepare 2.3% BSA (defatted) sol in 150mM NaCl (50ml) i.e., add 50mL of 150 mM NaCl solution by gentle shaking.
- Adjust the heat as needed to maintain the temperature at approx. 37˚C but not higher than 40˚C
- Stir until the BSA is completely dissolved and filter the BSA solution.
- Dilute the remaining filtered BSA solution with 25 mL of 150 mM NaCl solution, to make 0.17 mM stock.
- Aliquot into 4 mL glass vials and freeze at -20˚C for later use as a vehicle control

3) Preparing Palmitic acid (PA)/ Oleic acid (OA)Solution

OA was purchased from Sigma (Sigma-Aldrich, MO, USA, PA was purchased from Himedia. Prepare 10mM stock sol of PA/OA in 150 mM NaCl solution, by heating (37*C) & vortexing until clear. Place this flask in the beaker/ water bath and heat to 60'C while stirring.

4) Conjugating OA and BSA solution

- Make 2mM fatty acid aqueous sol of each, by adding 150mM NaCl. Heat (PA-70˚C/OA-60˚C) stir, until clear.

- Prepare fatty acid-BSA conjugate solution by mixing
- Transfer 20mL of the PA/OA solution to the 25ml BSA solution while stirring at 37˚C. Stir at 37˚C for 1 hour, monitoring the temperature of the water bath to keep between 35˚C and 40˚C.
- Adjust the final volume to 50 mL with 150 mM NaCl (2mM fatty acid solution + 0.34 mM BSA sol to get the 1mM final fatty acid conc and 0.17mM final BSA concentration, 6:1 FA: BSA).
- Check the pH and adjust it to 7.4 with 1N NaOH.
- Filter with 0.22micron filter and use for the experiments. Stable at -20 ˚C for 1 month.
- Heptadecanoic acid was dissolved in anhydrous ethanol and filtered, according to the standard protocol explained[16].

- **Protocol for MTT Assay (Oleic acid, Palmitic Acid and Heptadecanoic acid) on A549 cells.**

A549 cells were seeded in 96-well plates (1×10^4 cells per well) in low serum media (2%) overnight. After 24hrs, cells were treated with different concentration of standard fatty acids conjugated with BSA in a time dependant manner, also in low serum media and BSA vehicle control also in low serum media. Control wells (containing cells but not compounds), and the blank control (only medium) were plated with 5 replicates each.Untreated and treated cells were cultured at 37°C with 5% CO2 for 24 hours. MTT solution (5mg/ml) in media was added to each well and mixed; the wells were then incubated for an additional 4 hours.Culture supernatant was removed, DMSO (200 µl) was added to each well to fully dissolve the blue crystals. Absorbance was measured at 570 nm in a ELISA reade and the percentage of growth inhibition of A549 cells was calculated at each time point and for each concentration of PEB according to the following formulae:

% cell survival = (A570 Sanple – A570blank)/(A570negative – A570blank) × 100%

% cell growth inhibition = 1 - % cell survival.

Half maximal inhibitory concentration (IC50) values at respective times were then calculated using linear regression.

4.4.1.2 Characterization of effective fractions by Fourier-transform infrared spectroscopy (FTIR)

Principle

Fourier Transform-Infrared Spectroscopy (FTIR) is used to distinguish between organic and inorganic materials. This method plots the sample material's infrared radiation absorption against wavelength. The unknown IR absorption spectrum is compared to reference spectra in computer databases or to a spectrum acquired from a known substance in order to identify the substance being studied. Functional groups (such as -OH, C=O, N-H, CH3, etc.) are often responsible for absorption bands in the region of 4000 - 1500 wavenumbers.

Protocol

Dried powder of PEBE effective fraction was used for the FTIR analysis. To create translucent sample discs, 10 mg of dried powder was encapsulated in 100 mg of KBr pellet. All the powdered sample were loaded in FTIR spectroscope (BRUKER, FTIR spectrophotometer, Alpha II) with a scan range from 400 to 4000 cm^{12} with a resolution of cm- 1.

- Due to very less quantity of effective fraction, only FTIR was done as characterization method.

4.4.2 To study the effect purified fractions of CBE on H460 cell line and identification of phytocomponents by analytical methods.

4.4.2.1 Cytotoxic effect of fractions on H460 cells

The cytotoxic effect of all the isolated fractions from PEBE was checked on A549 cell line by MTT assay (as described in chapter 3, section 3.5.1.1).

4.4.2.2 Characterization of the effective purified fractions from CBE of *Bauhinia variegata*

The most cytotoxic purified fractions on H460 cells from CBE of *Bauhinia variegata* were characterized by: - **FT-IR, GCMS,^{1} H-NMR** and **HPLC** analysis.

4.4.2.2.1 To characterize the effective purified fractions from CBE using Spectroscopic Techniques (FTIR)

Protocol:

Dried powder of CBE purified fractions (PFF3-purified fraction F3 & PFF4-purified fraction F4) were used for the FTIR analysis. To create translucent sample discs, 10 mg of dried powder was encapsulated in 100 mg of KBr pellet. All the powdered sample (CBE purified

fractions) were loaded in FTIR spectroscope (BRUKER, FTIR spectrophotometer, Alpha II) with a scan range from 400 to 4000 cm^{12} with a resolution of cm- 1.

4.4.2.2.2 Gas Chromatography - Mass Spectrometry (GC-MS) analysis

GC-MS analysis of effective purified fractions (PFF3 and PFF4) were done at the Sophisticated Analytical Instrument Facility (SAIF) labs, IIT Bombay using standard GCMS model as explained below.

Instrument details

Agilent 7890 instrument was used for GC analysis, detector used was Flame Ionization Detector (FID) and the total run time of GC was 35 min.

Joel Accu Time of Flight Analyzer (TOF) GCV instrument for MS was used, Specification: Mass range of 10-2000 amu and mass resolution is of 6000.

GC-MS analysis was carried out by split less injection (spilt 1:10;80-1M-6-200-2M-8-275-10M-5-280-EA-HP5) of 1.0 µl of the sample in Ethyl acetate on a Hewlett Packard 6890 (USA) gas chromatograph integrated with a cross-linked 5% phenyl methyl Siloxane HP-5 MS capillary column (length 30 mm x internal diameter 0. 32 mm x film 0. 25 µm), joined with a mass detector.

Operating conditions for GC-MS

A 3minute hold period was used with a 35 °C initial column temperature. The temperature was set to increase by 8°C every minute, reaching a maximum of 280°C. A 1 ml/min flow of helium was used as the carrier gas to carry the sample down the column after it was introduced into the port in the procedure. At 70 eV, the MS spectrum was captured. Following the column separation, the components were recognised and subjected to additional analysis by FID. The compounds were identified by matching their spectra with those of known compounds in the NIST MS 2.0 structural database in order to determine their names, molecular weights, and structures.

4.4.2.2.3 Nuclear Magnetic Resonance (NMR) Spectroscopy

Application:

Nuclear magnetic resonance (NMR) spectroscopy is used in quality control and research to ascertain a sample's composition and purity as well as its molecular structure. NMR can be used to directly infer the fundamental structure of unknown substances or to compare against spectral libraries.

Characterization:

In conjunction with the Department of Chemistry at The Maharaja Sayajirao University, preliminary structural investigation of purified fractions (PFF3 & PFF4) utilising NMR spectroscopic techniques was completed. DMSO-d6 was used as the solvent system to record the NMR spectra (1H NMR) at 400 MHz using Bruker AVIII 400 MHz NMR spectrometers. Chemical shift (ppm), multiplicity (singlet, doublet, triplet, quartet, and multiplet), coupling constant (Hz), integration, and assignment are the data for 1H NMR that are recorded. After 100% assignment of the most abundant ion, the mass spectrometry was utilised to determine the mass to charge measurement.

4.4.2.2.4 High performance liquid chromatography (HPLC) Analysis

The Agilent 1200 system (Palo Alto, CA, USA) was used for the HPLC analyses. It includes a quadruple pump, autosampler, and PDA SP40 diode array detector (DAD). The column was a Zorbax C18 from Agilent (150 x 4.6 mm i.d., 5 m particle size). HPLC grade methanol and deionized water (90:10, v/v) were combined in the mobile phase, at a flow rate of with a flow rate of 0.5 mL/min and a column temperature of 25°C. Samples (PFF3 &PFF4) were prepared by dissolving the dried fractions in HPLC grade methanol. Each sample solutions were filtered using 0.45µm filter before injecting into HPLC system. UV detection was done at 280nm. The injection volume of sample solution was 20µl. The peaks in the chromatogram were compared by the retention time and UV spectra of standard compounds.

4.5 Results and Discussion

4.5.1 Identification, characterization and cytotoxic effect of the effective phytocomponents of PEBE on A549 cell line.

The Column Chromatography of the PEBE lead to extraction of 91 fractions which was further pooled down into nine sub-fractions, followed by Thin Layer Chromatography to find individual Retardation Factor (Rf value) as explained above in 4.3.1.1. Further, **MTT assay** was performed on A549 with all the nine isolated fractions from PEBE and it was found that the most cytotoxic fraction of PEBE on A549 cell is P8 for 48h as shown in Figure 4.7.

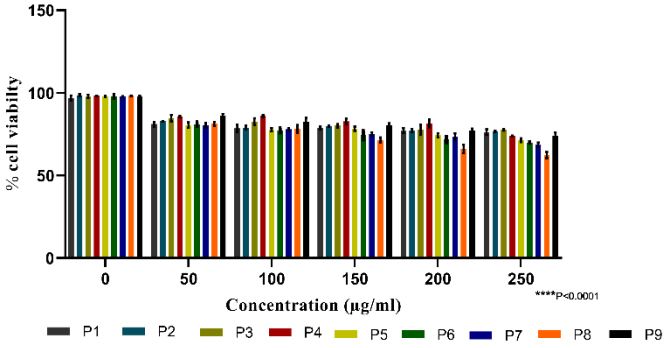

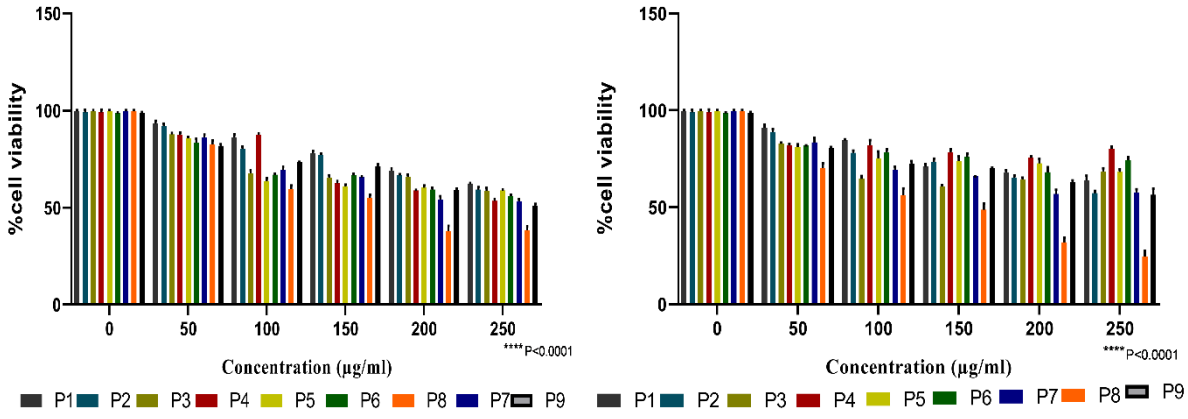

Figure 4.7 Effect of fractions of PEBE on A549 cell line at a) 24 h b) 48 h c) 72 h.

4.5.1.1 Characterization of effective fractions of PEBE by Fourier-transform infrared spectroscopy (FTIR)

The data on the peak values and the possible functional groups (obtained by FTIR analysis) present in the P8 fraction of *Bauhinia variegata* are presented in Figure 4.8 and table 3. The wavenumber 3000-2500 cm^{-1}showing highest peak corresponds to the lipids. The absorption peak at 2926.37 and 2854.13 cm^{-1} corresponds to O-H stretch (carboxylic acids) for all derivatives, -CHO group. The absorption peak 1733-1710 cm^{-1} corresponds to C=O carbonyl group. The absorption peak 1687.50 corresponds to C=N groups. The absorption peak at 1461.85 corresponds to C=C-C, Aromatic ring stretch (Aromatic compound). The absorption peak at 1375.96 corresponds to C-O stretching. The absorption peak at 1237.26–1133.93 cm^{-1} corresponds to C-O stretching. The absorption peak at 883.47- 722.16 corresponds to C=C stretching. **As the concentration increase, transmittance decreases**, so lipids concentration is higher in fraction P8.

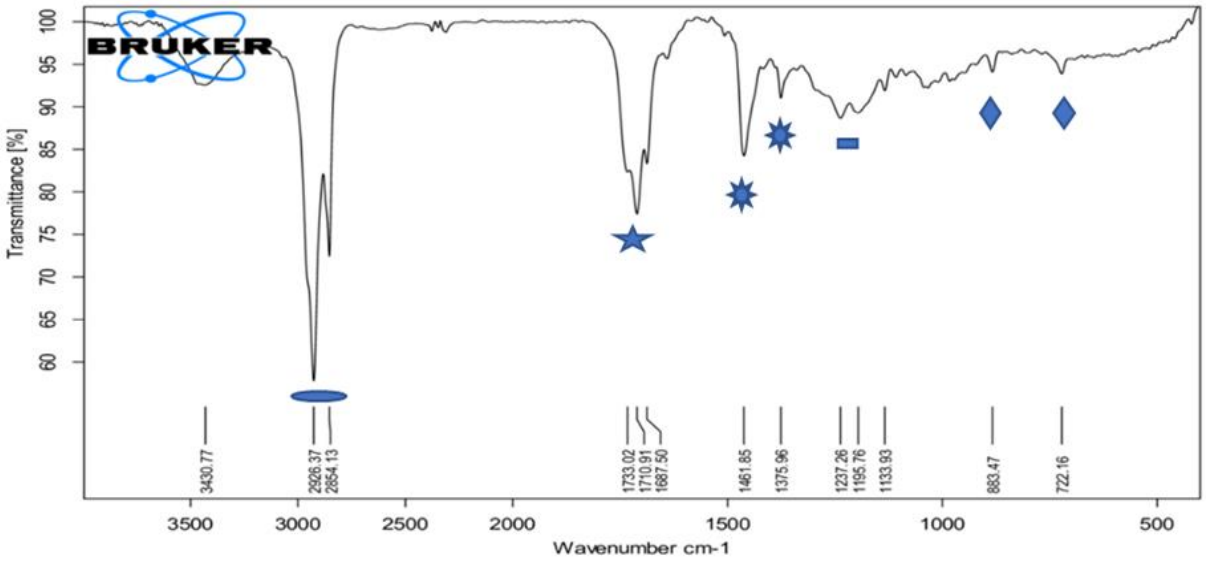

Figure 4.8 The FTIR profile of fraction P8 showed the wave number corresponding to different compounds.

Table 4.3 FTIR spectral peak values and type of groups obtained for the P8 fraction of PEBE of *Bauhinia variegata*.

WAVE NUMBERS	TYPE
3000 - 2500 (2926.37, 2854.13)	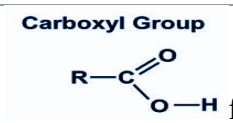 for all derivatives Lipids
1740 – 1710 (1710.91, 1687.50)	C=O carbonyl group
1395 – 1475 (1461.85, 1375. 96)	Aromatic ring stretch, C=O stretching
1240 – 1200 (1237.26, 1195.76)	C-O stretching
883.47 and 722.16	C=C stretching

4.5.1.2 To check the effect of active pytocomponents from PEBE on A549 cell line by MTT assay

P8 fraction was found to be most cytotoxic among all fractions as explained above. But due to very small quantity of effective fraction P8 of PEBE, there was difficulty in further separating as well as working with these compounds, so further experiments were carried out with standards of these compound. **The compounds** [Heptadecanoic acid (28%), Oleic acid (10.47%), and n-hexadecanoic acid (Palmitic acid) (1%)] were chosen for further experiments based on their percentages present in the Petroleum ether bark extract (by GC/MS) as well as in fraction P8 (by FTIR) and by considering the literature studies[13,14,15,16,17,18,19] which report anticancer properties of these compounds. Preparation of these selected compounds is explained above in (section 4.4.1.1.1).

Table 4.4 Percentage profile of compounds found in the petroleum ether bark extract (PEBE) through GC/MS:

SI. No.	RT (min.)	Name of compound	Molecular formula	Molecular weight	CAS	Peak %

1.	23.46 min.	n-hexadecenoic acid	$C_{16}H_{32}O_2$	256	57-10-3	1%
2.	25.04 min.	Oleic acid	$C_{18}H_{34}O_2$	282	112-80-1	2.33%
3.	25.96 min.	Oleic acid	$C_{18}H_{34}O_2$	282	112-80-1	5.2%
4.	27.38 min.	Oleic acid	$C_{18}H_{34}O_2$	282	112-80-1	2.94% = (2.33%+5.23%+2.94%= 10.47%)
5.	29.88 min.	Heptadecanoicacid	$C_{17}H_{34}O_2$	270	506-12-7	4.9%

The percentage of all compounds in the extract were calculated from GS-MS profile as

% of compound = Area of the individual compound under the curve/ Total area under the curve of the all compounds.

These compounds were choosen for further studies on 549 cells.

4.5.1.2.1 Cytotoxic effect of Oleic acid on A549 cells

MTT assay was performed to examine the effect of oleic acid (OA) on the proliferation of A549 cells. The anti-proliferative effect of Oleic acid on A549 cells was observed in a dose and time dependent manner. Oleic acid significantly decreases the proliferation of A549 cells in a dose- dependent manner for 24h, 48h and 72h as shown in Figure 4.9 (a, b, c).

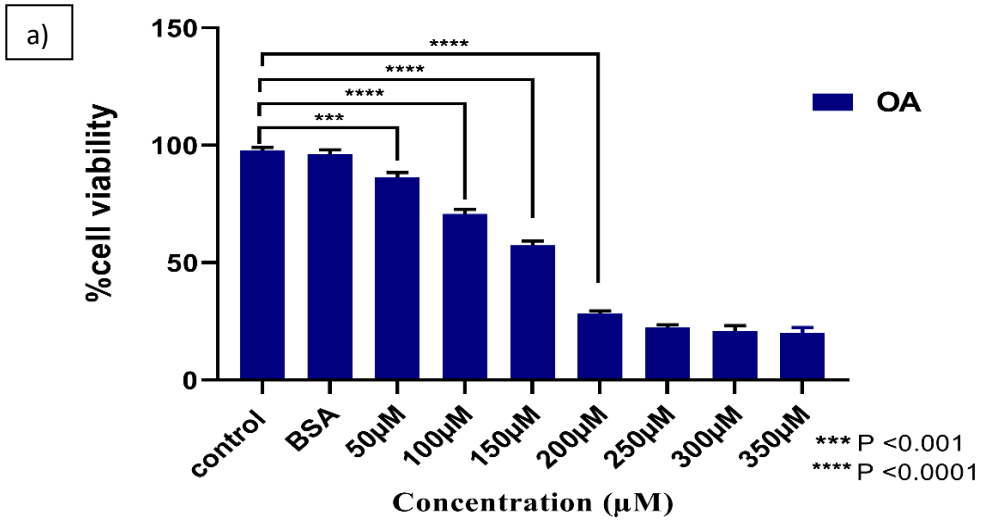

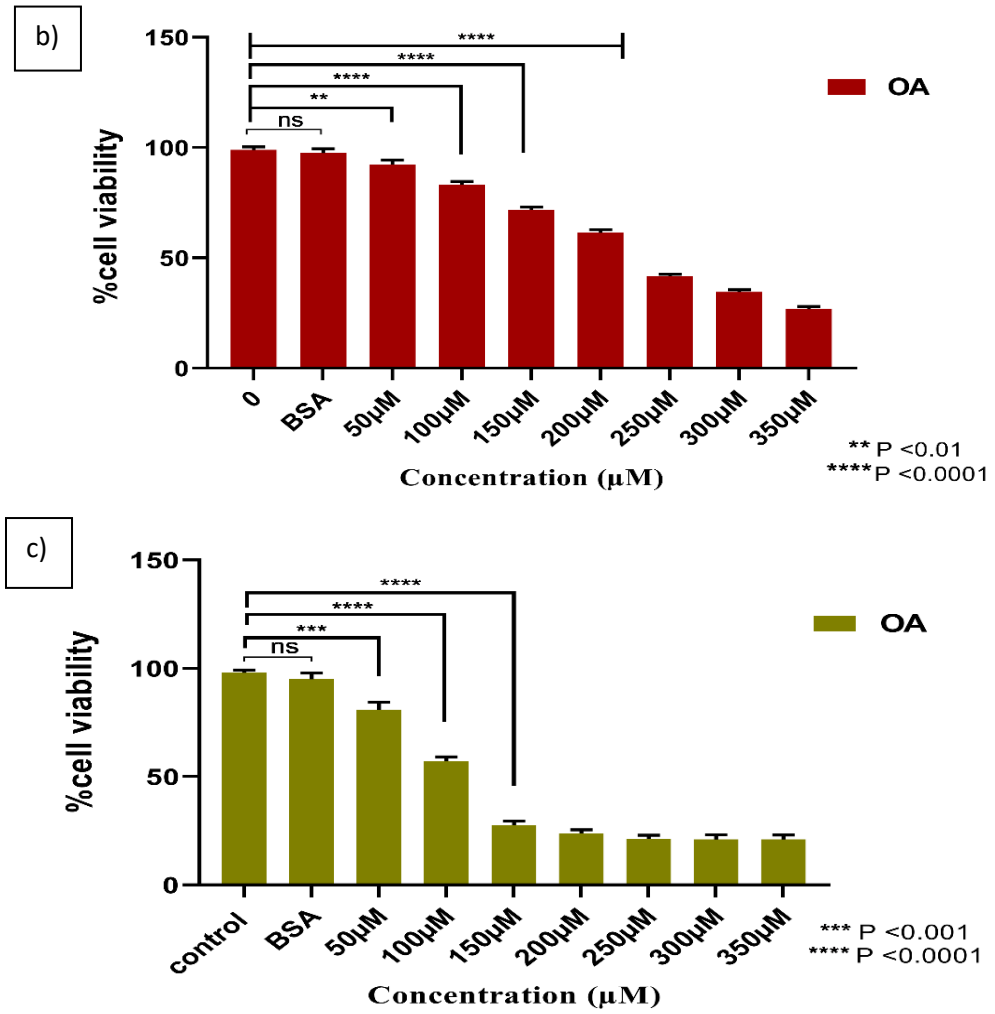

Figure 4.9 The effect of Oleic acid on A549 cell line for 24 h, 48 h and 72 h. **(a)** Effect of different concentrations of Oleic acid on A549 cells for 24 h **(b)** Effect of different concentrations of Oleic acid on A549 cells for 48 h **(c)** Effect of different concentrations of Oleic acid on A549 cells for 72 h respectively. Data represented as the mean± standard deviation of at least three experiments. *P<0.05, **P<0.01, ***P<0.001, ****P<0.0001.

4.5.1.2.2 Cytotoxic effect of Palmitic acid on A549 cells

The anti-proliferative effect of Palmitic acid (PA) on A549 cells was observed in a dose and time dependent manner. Palmitic acid showed no significant increase in cell death even after a time period of 72 hours, as shown in Figure 4.10 (a, b, c). Some literature studies suggest, palmitic acid promote proliferation[20] and cause lung metastasis of melanomas after PA treatment[21].

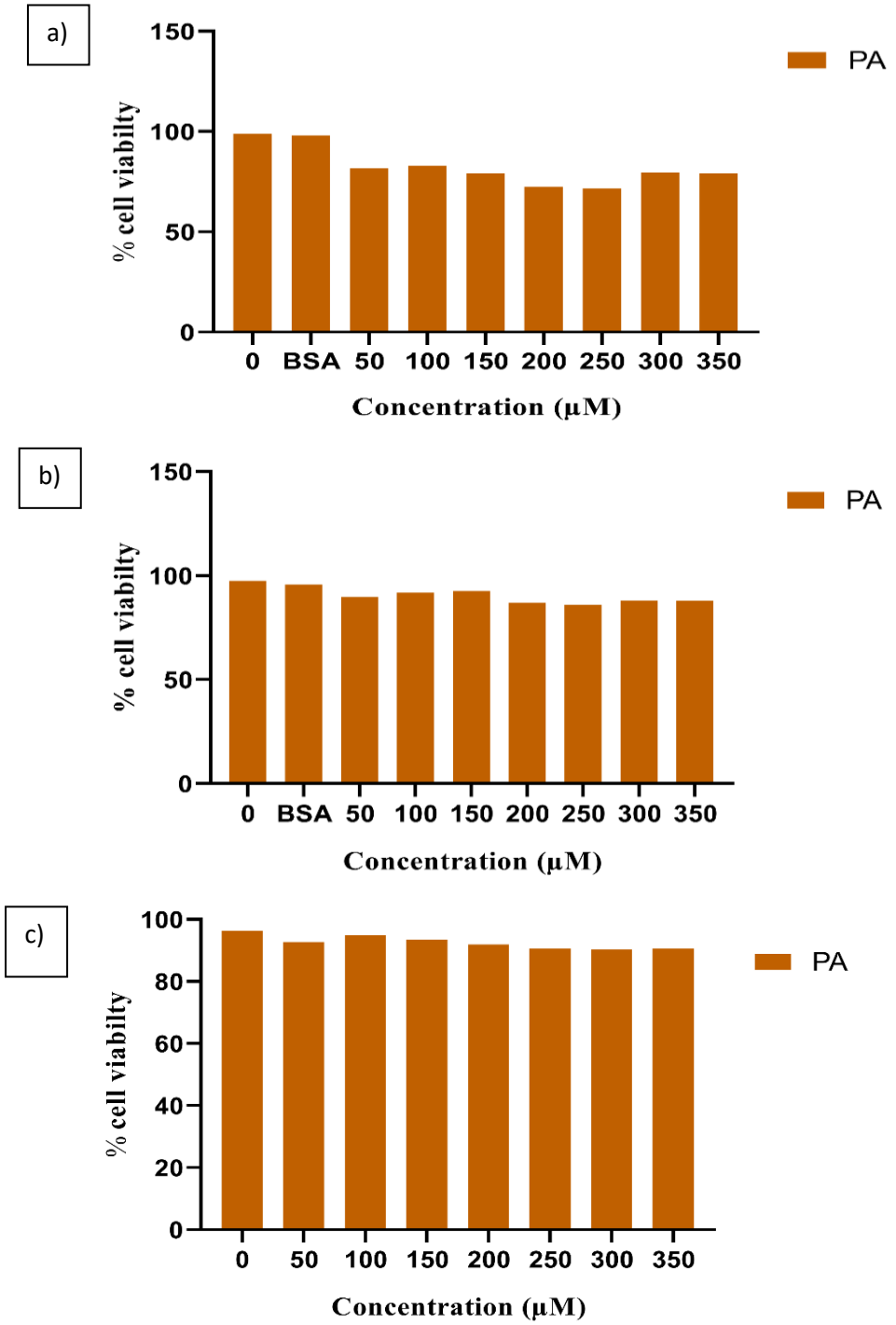

Figure 4.10 The effect of Palmitic acid against A549 cell line for 24 h, 48 h and 72 h. **(a)** Effect of different concentrations of Palmitic acid on A549 cells for 24 h **(b)** Effect of different concentrations of Palmitic acid on A549 cells for 48 h **(c)** Effect of different concentrations of Palmitic acid on A549 cells for 72 h respectively.

4.5.1.2.3 Cytotoxic effect of Heptadecanoic acid on A549 cells

The anti-proliferative effect of Heptadecanoic acid (HD) on A549 cells was observed in a dose and time dependent manner. There was effective and significant cytotoxic effect observed

after treating A549 cells with Heptadecanoic acid after 72hrs with defined concentrations.

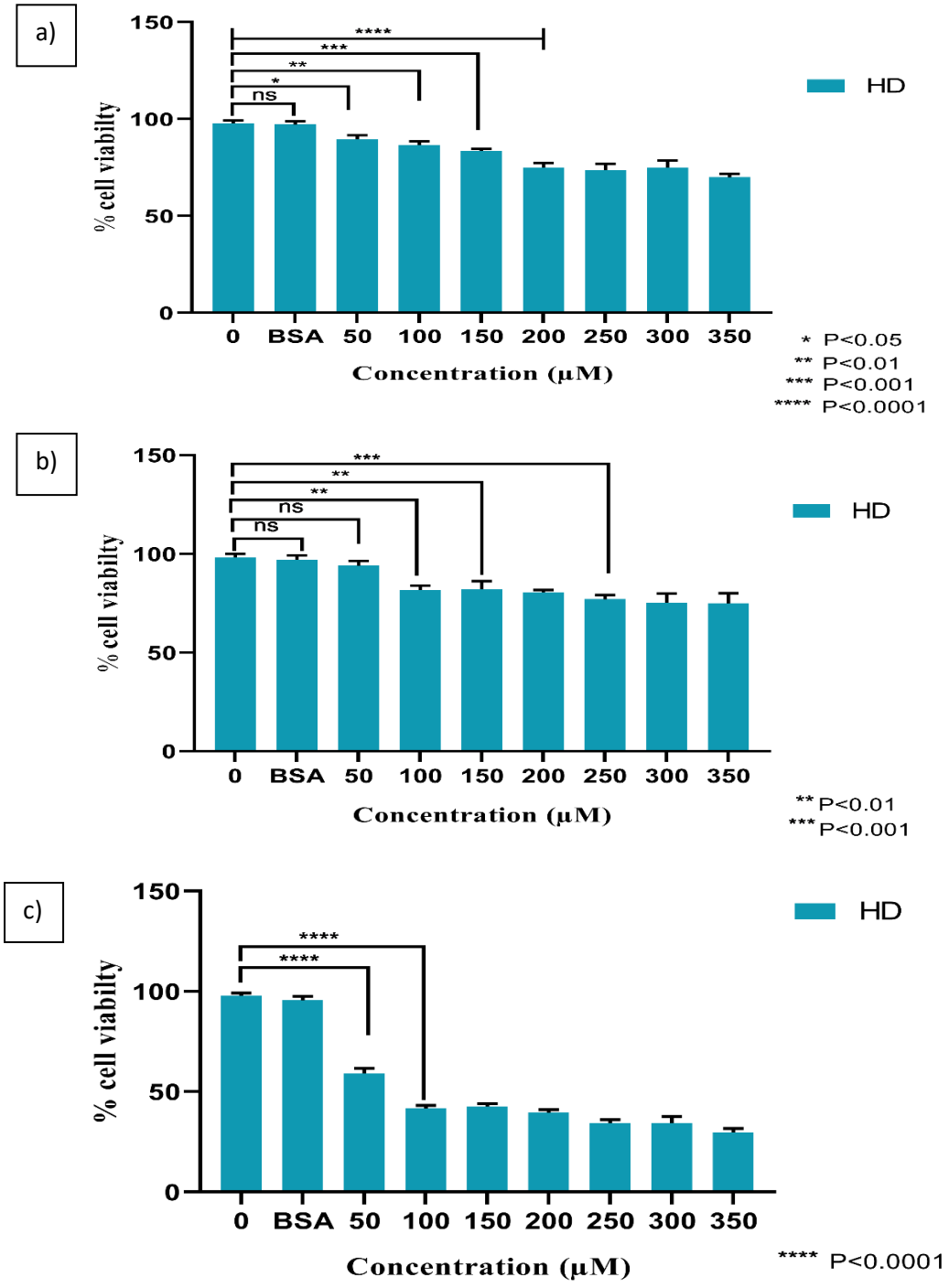

Figure 4.11 The effect of Heptadecanoic acid on A549 cell line for 24 h, 48 h and 72 h. **(a)** Effect of different concentrations of Heptadecanoic acid on A549 cells for 24 h **(b)** Effect of different concentrations of Heptadecanoic acid on A549 cells for 48 h **(c)** Effect of different concentrations of Heptadecanoic acid on A549 cells for 72 h respectively.

Cytotoxic effect of Oleic acid, Palmitic acid and Heptadecanoic acid was checked on A549 cells in dose and time dependent manner (as explained above). Oleic acid showed to be most effective on A549 cells. So, further experiments were carried out with Oleic acid.

4.5.1.2.4 Determination of IC50 Value of Oleic acids

Effect of different concentrations of Oleic acid on the viability of A549 cells for different time measure (at 24 h, 48 h and 72 h) was assessed. The IC50 values were 230µM for 24 h, 150µM for 48 h and 148µM for 72 h as shown in Figure 4.12 (a, b, c). Oleic acid was more potent after 48 h treatment with 150 µM concentration; hence this time point was selected for further experiments.

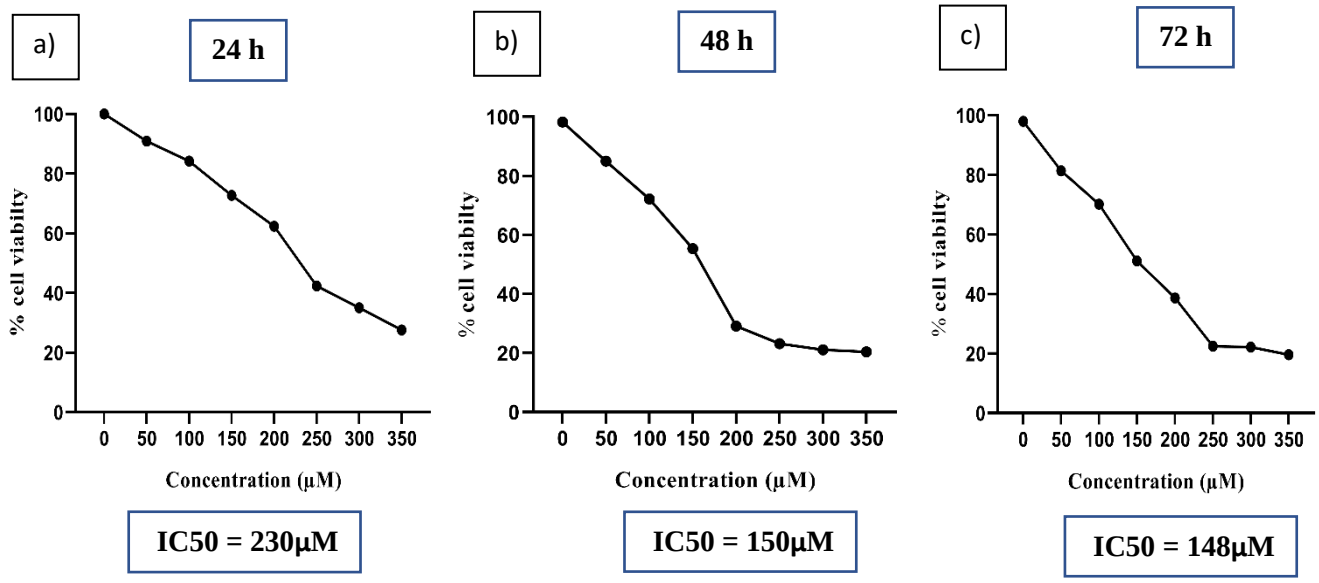

Figure 4.12 IC50 values of Oleic Acid on A549 cells at a) 24h, b) 48h and c) 72h.

4.5.1.2.4.1 Oleic Acid Inhibit Growth and Proliferation of A549 Cells

The morphological examination of the A549 cells after Oleic acid treatment after 48h showed cell shrinkage and rounding up of the cells which are typical features of cell death as shown in Figure 4.13

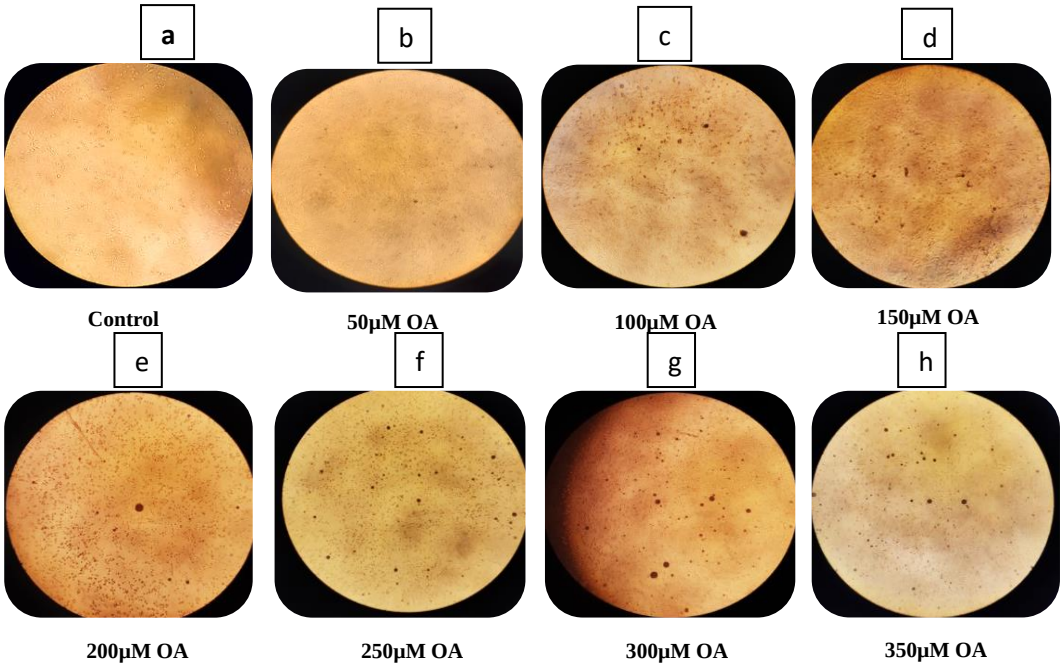

Figure 4.13 Morphological images of A549 cells (a) without treatment and cells exposed to (b) OA (50µM), (c) OA (100 µM), (d) OA (150 µM), (e) OA(200 µM), (f) OA (250 µM), (g) OA (300 µM), (h) 350 (µM).

4.5.2 To study the effect of purified fractions of CBE on H460 cell line and identification of phytocomponents by analytical methods.

4.5.2.1 Screening of bioactive fractions for the cytotoxic effect on H460 cells

The cytotoxic effect of all the purified fractions (F1 to F9) obtained by column chromatography of Chloroform bark extract (as explained above in table 2) of *Bauhinia variegata* were assessed against H460 cell line for 24h, 48h and 72h. The effect of H460 cells to increasing concentrations of different fractions are shown in Figure 4.14. The results showed that the viability of H460 cells decreased in a dose and time-dependent manner with an increase in concentration of some fractions. **Purified fractions F3 (PFF3) and F4 (PFF4)** of CBE of *Bauhinia variegata* exhibited a cytotoxic potential against H460 cells in a dose and time dependent manner, then all other fractions.

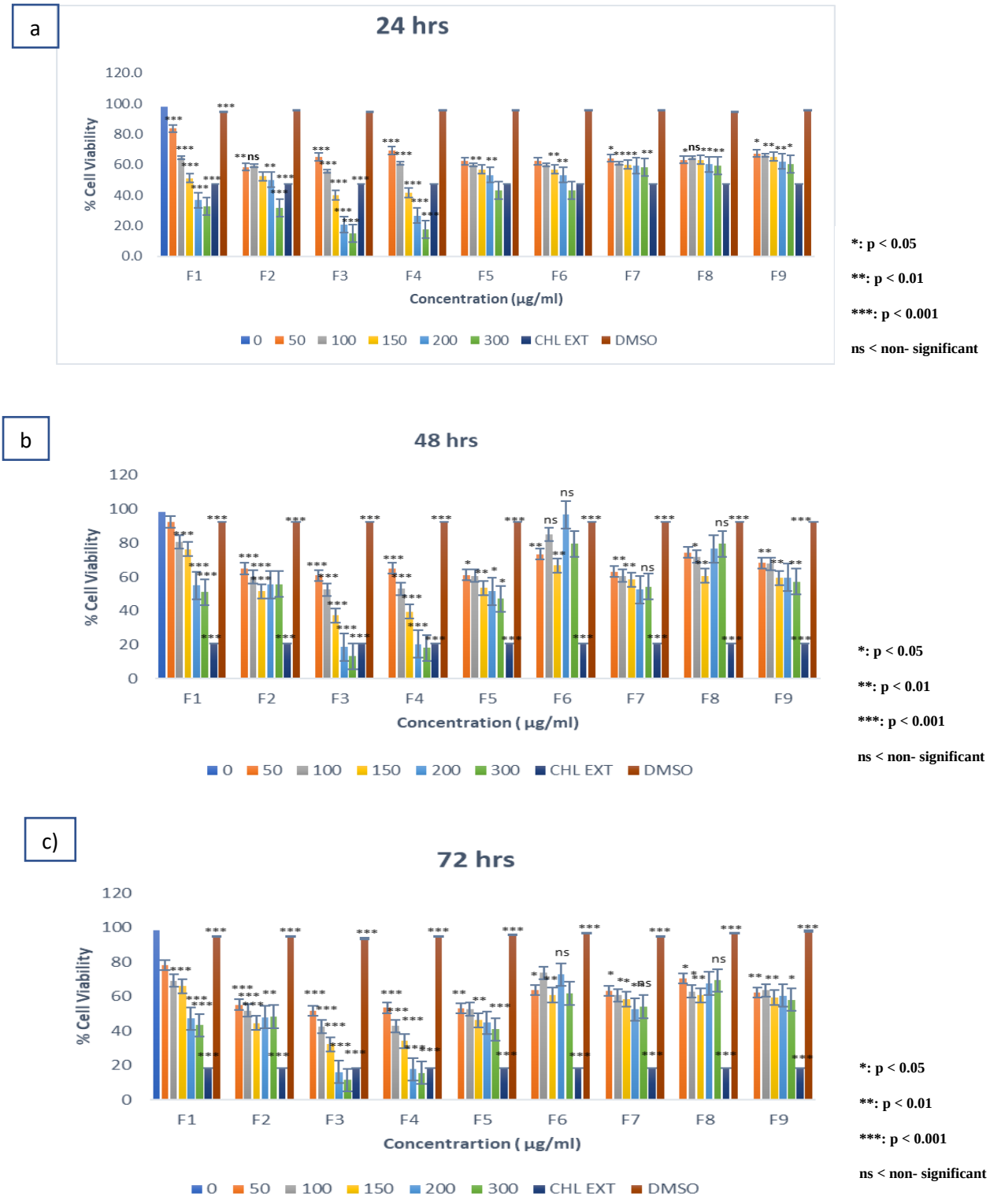

Figure 4.14 The effect of CBE fractions (F1to F9) against H460 cell line for 24 h, 48 h and 72 h. **(a)** Effect of different concentrations of different fractions on H460 cells for 24 h **(b)** Effect of different concentrations of different fractions on H460 cells for 48 h **(c)** Effect of different concentrations of different fractions on H460 cells for 72 h respectively. Data represented as the mean± standard deviation of at least three experiments. *P<0.05, **P<0.01, ***P<0.001, ****P<0.0001.

4.5.2.2 Determination of IC50 values of PFF3 and PFF4

Effect of different concentrations of **PFF3 and PFF4**, on the viability of H460 cells for different time measure (at 24 h, 48 h and 72 h) was assessed. The IC50 values were for 24 h, for 48 h and for 72 h as shown in Figure 4.15(a, b, c). PFF3 and PFF4 were more potent after 24 h treatment; hence this time point was selected for further experiments.

a)

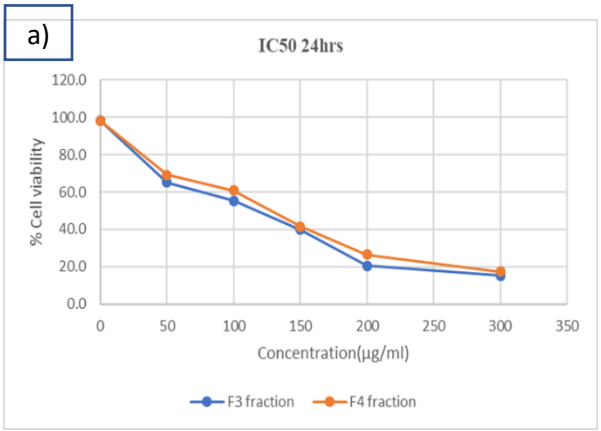

PFF3 IC50=120µg/ml | **PFF4 IC50= 130µg/ml**

b)

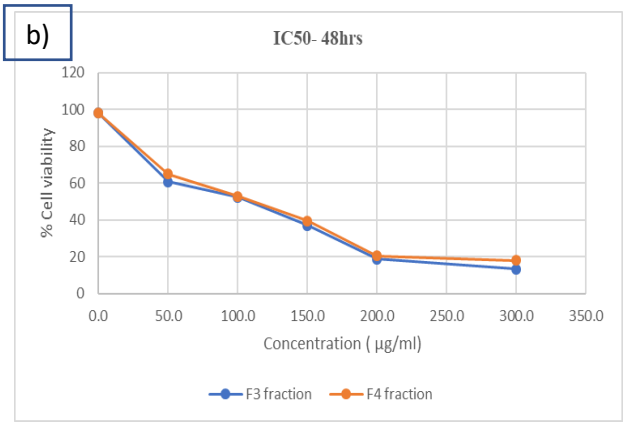

PFF3 IC50=100µg/ml | **PFF4 IC50= 100µg/ml**

c)

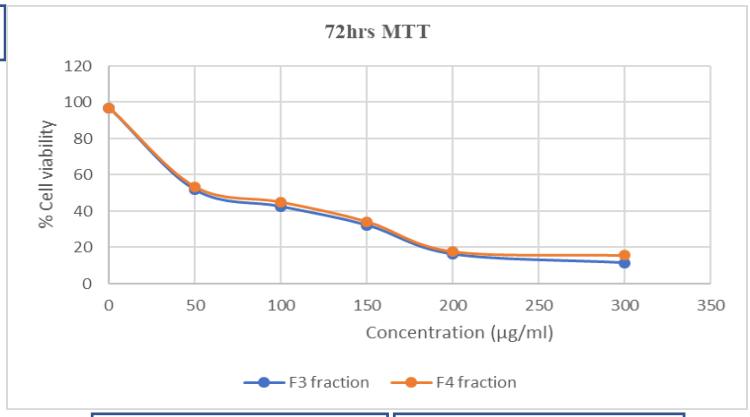

PFF3 IC50= 90µg/ml | **PFF4 IC50= 90µg/ml**

Figure 4.15 IC50 values of PFF3 and PFF4 on H460 cells at a) 24h, b) 48h and c) 72h.

As there was not much difference in the IC50 value of PFF3 & PFF4 at 24hr, 48hr & 72hr treatment, therefore 24hrs treatment with IC50 of 120µg/ml for PFF3 & IC50 of 130µg/ml for PFF4 was used for further experiments.

4.5.2.2.1 PFF3 Inhibit Growth and Proliferation of H460 Cells

The morphological examination of the H460 cells after PFF3 treatment at different concentrations after 24h showed cell shrinkage and rounding up of the cells which are typical features of cell death as shown in Figure 4.16

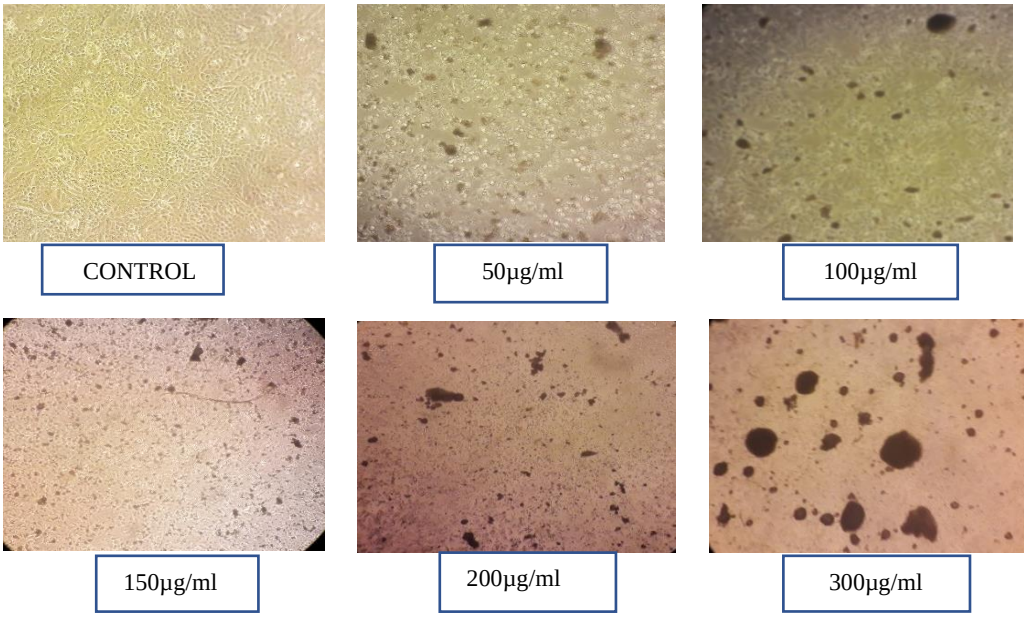

Figure 4.16 Microscopic images of H460 cells treated with PFF3 at different concentrations for 24 hours. The black dots represent apoptosis of cells treated with PFF3.

4.5.2.2.2 PFF4 Inhibit Growth and Proliferation of H460 Cells

The morphological examination of H460 cells after PFF4 treatment at different concentrations after 24h showed cell shrinkage and rounding up of the cells which are typical features of cell death as shown in Figure 4.17.

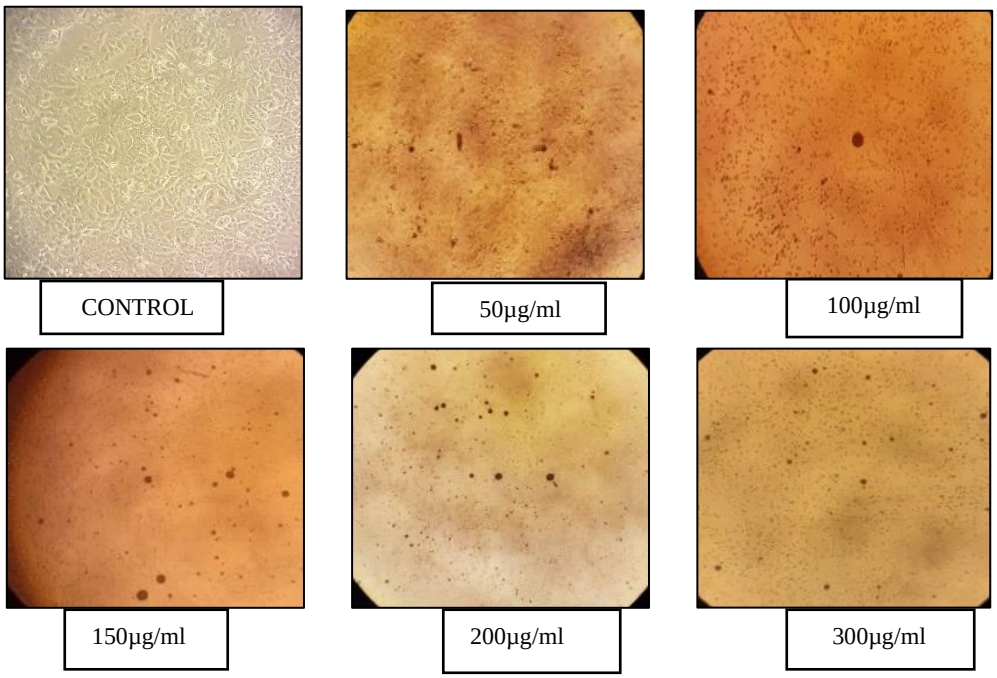

Figure 4.17 Microscopic images of H460 cells treated with PFF4 at different concentrations for 24 hours. The black dots represent apoptosis of cells treated with PFF4 (100x magnification).

4.5.2.2.3 Characterization of PFF3 and PFF4 from CBE of *Bauhinia variegata* by:

4.5.2.2.3.1 Characterization of PFF3 & PFF4 using FTIR

a) FTIR Image of PFF3

The data on the peak values and the possible functional groups (obtained by FTIR analysis) present in PFF3 are presented in Figure 4.18 and table 4. The IR spectra of PFF3 showed absorption peaks from CH3 and CH2 stretching and C-H bending at 2925.98 and 2854.93 cm^{-1}, 1461.62 respectively. The typical carbonyl peak was observed at 1709 cm^{-1}. Absorption peak at 1216.06 cm^{-1} were allotted to symmetrical bending in C-H and C-N (aryl) stretching. Peak at 759.42 cm^{-1} corresponds to C=C bending and 669 cm^{-1} to halo compounds.

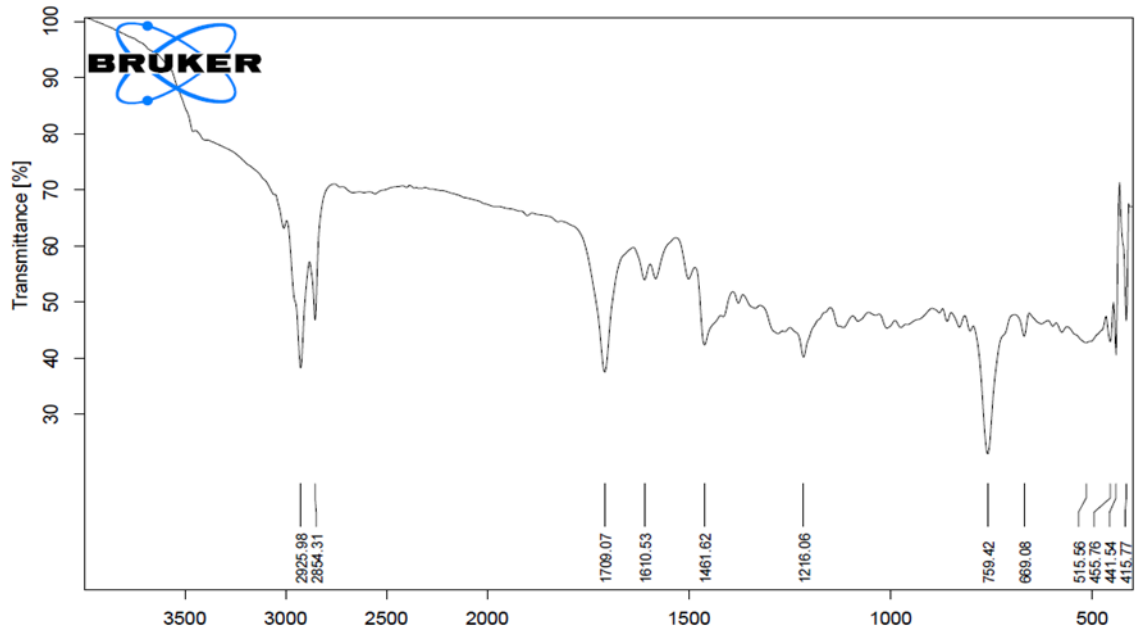

Figure 4.18 The FTIR profile of PFF3 showed the wave number corresponding to different compounds.

Table 4.5 FTIR spectral peak values and type of groups obtained for the PFF3 of CBE of *Bauhinia variegata*.

Peak values	Functional groups
669.35	halo compounds
759.42	C=C bending
1216.06	C-H stretching, alkyl aryl ether
1461.62	C-H stretching
1709.07	C=O stretching, carboxylic acid
2854.93	-OH group, CHO group
2925.98	C-H stretching

b) FTIR Image of PFF4

The data on the peak values and the possible functional groups (obtained by FTIR analysis) present in the PFF4 are presented in Figure 4.19 and table 5. The IR spectra of PFF4 showed absorption peaks of CH3 and CH2 stretching and C-H bending at 2921.13 and 2852.06 cm^{-1}, 1462.85 respectively. The typical carbonyl peak was observed at 1708.76 cm^{-1}. Absorption peak at 1214.95 cm^{-1} corresponds to C-O stretching. Peak at 759.42 cm^{-1} corresponds to C=C bending.

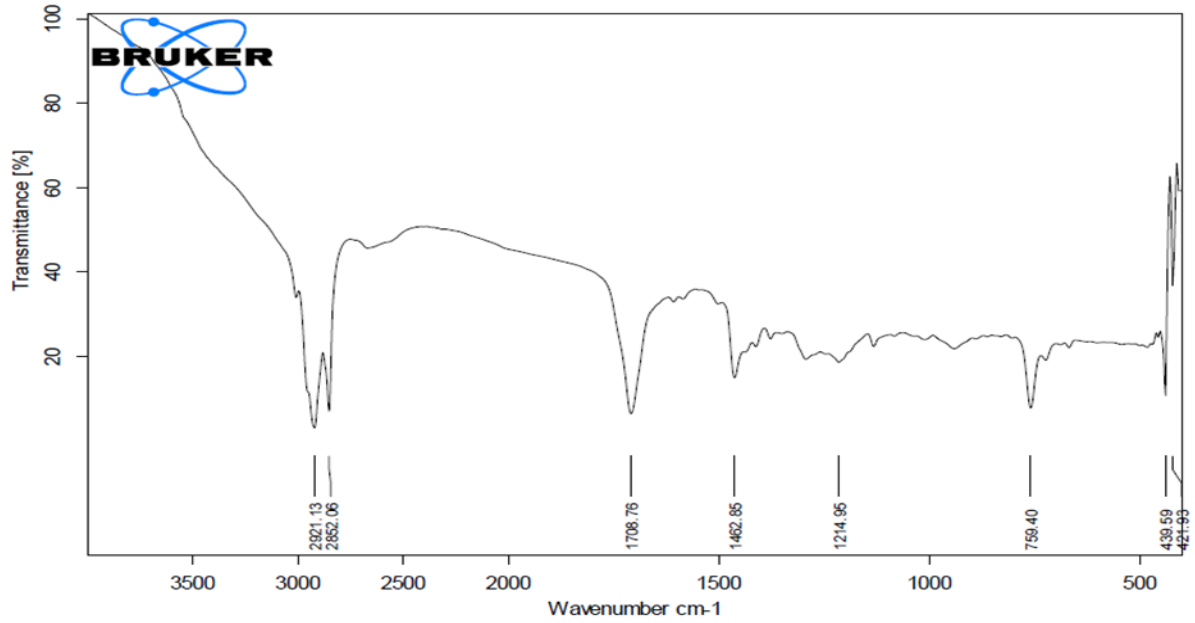

Figure 4.19 The FTIR profile of PFF4 showed the wave number corresponding to different compounds

Table 4.6. FTIR spectral peak values and type of groups obtained for PFF4 of CBE of *Bauhinia variegata*.

Peak values	Functional groups
759.40	C-H bending
1214.95	C-O streching
1462.85	C-H stretching
1708.76	C=O carbonyl group
2852.06	-OH group
2921.13	C-H stretching

- The presence of carbonyl groups and few others functional groups was confirmed by Fourier-transform infrared spectroscopy (FTIR).
- By evaluating functional groups found in FTIR data & by looking into previous GC-MS results of CBE, we can conclude that maybe mixture of compounds can be present in the PFF3 & PFF4 of CBE of *Bauhinia variegata*.

4.5.2.2.3.2 Gas Chromatography - Mass Spectrometry (GC-MS) analysis

a) GC/MS analysis of PFF3

GC/MS analysis of PFF3 and PFF4 was performed for the identification of unknown compounds. The detailed list of phytocomponents identified in the **PFF3** of CBE of *Bauhinia variegata* along with the corresponding retention time, name of the compound, CAS number of the compound, molecular formula as well as their relative abundance, which was expressed in terms of peak area% are presented in Table 6.

Table 4.7. Phytochemical constituents identified in the PFF3 using gas chromatography-mass spectrometry. CAS: chemical abstract service

S.No.	Retention time	Name of Compound	Molecular formula	CAS	% compound total
1.	15.06	Phenol,2,4-bis(1,1dimethylethyl)	$C_{14}H_{22}O$	96-76-4	0.18
2.	16.13	Dodecanoic acid	$C1_2H_{24}O2$	143-07-7	0.12

3.	16.30	3-Tetradecene, (Z)	$C1_4H_{28}$	41446-67-7	0.13
4.	19.79	Tetra decanoic acid	$C_{14}H_{28}O_2$	544-63-8	0.37
5.	19.98	1- Hexadecene	$C_{16}H_{32}$	629-73-2	0.31
6.	21.02	Nickel, [5,10,15,20-tetrakis(4-methoxyphenyl)-21H,23H-prophinato (2-)-N21, N22, N23, N24], (SP-4-1)	$C_{48}H_{36}N_4NiO_4$	39828-57-4	0.091
7.	21.26	Oxacyclotetradecane-2,11-dione,13-methyl	$C_{14}H_{24}O_3$	74685-36-2	0.39
8.	21.54	Pentadecanoic acid	$C_{15}H_{30}O_2$	1002-84-2	0.45
9.	24.21	**n-Hexadecanoic acid**	$C1_6H_{32}O_2$	57-10-3	**20.3**
10.	25.22	**n- Hexadecanoic acid**	**$C_{16}H_{32}O_2$**	**57-10-3**	**0.28**
11.	25.56	**n- Hexadecanoic acid (Palmitic acid)**	**$C1_6H_{32}O_2$**	**57-10-3**	**0.49**
12.	27.30	**9,12-Octadecadienoic acid [Z, Z] (Linoleic acid)**	**$C_{18}H_{32}O_2$**	**60-33-3**	**35.45**
13.	28.56	9,12,15-Octadecatrienoic acid,2[trimethylsilyl) oxy]-1-[trimethylsilyl) oxy]-methyl], ethyl ester, [Z, Z, Z]	$C_{27}H_{52}O_4Si_2$	55521-23-8	0.24
14.	28.87	Fenofibrate	$C_{20}H_{21}ClO_4$	49562-28-9	1.19
15.	29.85	1-Eicosanol	$C_{20}H_{42}O$	629-96-9	0.44
16.	30.04	Z-7_hexadecenoic acid	$C_{16}H_{30}O2$	130908	0.43
17.	31.62	Cyclodecasiloxane, eicosamethyl-	$C_{20}H_{60}O_{10}Si_{10}$	18772-36-6	0.34
18.	32.04	1-Eicosanol	$C_{20}H_{42}O$	629-96-9	0.37
19.	32.69	1,1-2,2-Bis[2,3-dimethylbenzoquinonyl]	$C_{16}H_{16}O_4$	98108-02-2	0.90

20.	32.85	4-(1,1-dimethylallyl]-9 methoxy-7H-furo[3,2-g] [1] benzopyran-7-one	$C_{17}H_{16}O_4$	34155-80-1	2.03
21.	33.59	**4-Hydroxy-9-(3-methyl-2-butenyl) furo (3,2-g) chromen-7-one (Alloisoimperatorin)**	**$C_{16}H_{14}O_4$**	**35214-83-6**	**31.39**
22.	33.67	10,11-dihydro-2,3,6-trimethoxydibenz(b,f)oxepin-10-one	$C_{17}H_{16}O_5$	19172-30-6	2.86
23.	33.95	Glycine, N-[3α,5β]-24-oxo-3[(trimethylsilyl)oxy) cholan-24-yl]-, methyl ester	$C_{30}H_{53}NO_4Si$	57326-15-5	0.315
24.	39.25	Stigmasta-5,22-diene-3-ol, acetate, (3β)-	$C_{31}H_{50}O_2$	4651-48-3	0.23
25.	40.60	9-Octadecanoic acid (Z)-,2-hydroxy-1-(hydroxy methyl)ethyl ester	C21H40O4	3443-84-3	0.45

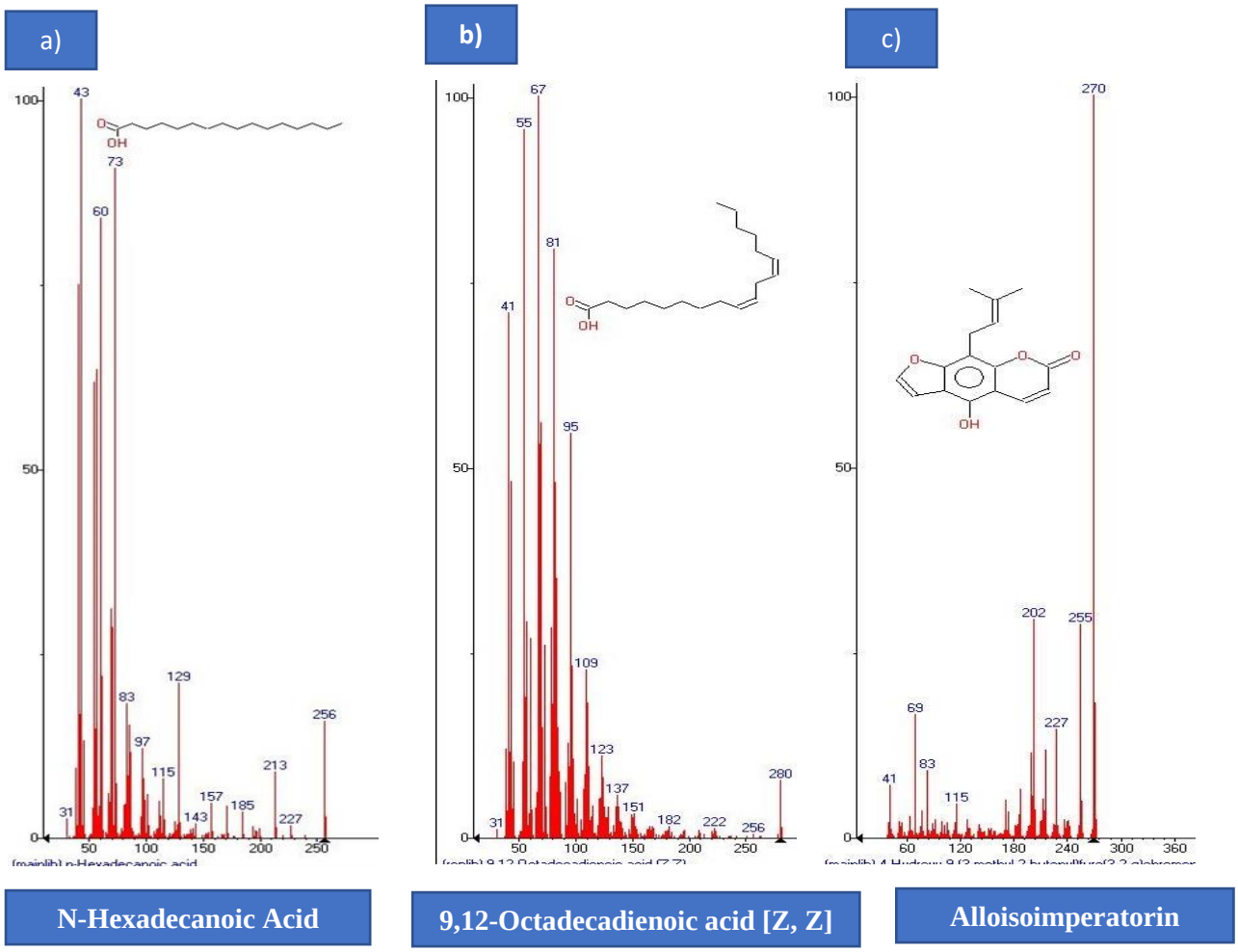

Figure 4.20 Product ion spectrum stating the structure of the major phytocomponents (by %) identified in purified fraction F3 **(PFF3)** by GC/MS and NIST Library in [A] n-Hexadecanoic acid [B] Palmitic acid [C] Alloisoimperatorin.

- **A total of 22 compounds were identified in PFF3 by GC-MS. Palmitic acid (21.07%), Linoleic acid (35.45%) and Alloisoimperatorin (31.39%) accounting for 87.68% of the total area, were the main compounds identified in PFF3.**

The size of the peak area in a GC-MS chromatogram does not necessarily correlate with the biological activity of a compound. While a compound with a larger peak area may be present in higher abundance in the sample, it may not be the active component responsible for the observed biological effect.

Though, many studies have confirmed that these phytocomponents (**Palmitic acid (PA)**, **linoleic acid (LA)** and **Alloisoimperatorin**) possess various anti-cancerous properties.

Literature studies showed that **Palmitic acid (PA)** prevents cell proliferation and induces apoptosis of human gastric cancer cells[15,18]. In prostate cancer, dietary palmitic acid encourages tumour development and epithelial-mesenchymal transition[20,21]. Palmitic acid increase the sensitivity of cancer cells to specific anti- cancer compound and induce apoptosis[22]. PA prevents cell proliferation as well as cause cell death depending upon the cell type, duration and concentration of treatment[23].

Literature studies showed that **linoleic acid (LA)** inhibit tumour cell growth as well as promote proliferation of cancer cells depending upon the cell type and the concentration[24.25].It has been shown that Linoleic acid decrease human lung-tumour cell growth in a concentration-dependent manner[26,27].

Literature studies also showed that **Alloisoimperatorin** is a coumarin derivative that has been reported to have anti-inflammatory and anticancer properties[28,29,].

Further, to check the effect of LA and PA on H460 cells, MTT assay was performed with standards of Linoleic acid (LA) and Palmitic acid (PA) in a concentration and time-dependent manner. Our results showed that LA promote lung cancer cell growth, only the highest concentration slightly showed anti-proliferative effect on H460 cells at 24h. So, LA is not showing cytotoxic effect at the defined concentrations of **PFF3** (explained above in 4.5.5.2) on H460 cells. Further, Palmitic acid showed cytotoxic effect on H460 cells at 24h in a concentration dependent manner. Palmitic acid showed more cytotoxic effect at higher concentrations than at lower concentrations at 24h on H460 cells. **So, it can be concluded that phytocomponents in PFF3 might be working synergistically with each other and showing cytotoxic effect on H460 cells. Therefore, compound(s) from purified Fraction-F3 can be used for the chemoprevention and treatment of lung cancer.**

b) GC/MS analysis of PFF4

GC/MS analysis of PFF4 was performed. The detailed list of phytocomponents identified in the **PFF4,** along with the corresponding retention time, name of the compound, CAS number of the compound, molecular formula as well as their relative abundance, which was expressed in terms of peak area% are presented in Table 7.

Table 4.8. Phytochemical constituents identified in the PFF4 using gas chromatography-mass spectrometry. CAS: chemical abstract service

S.No.	Retention time	Name of Compound	Molecular formula	CAS	% compound total
1.	23.6	N-hexadecanoic acid	$C_{16}H_{32}O_2$	57-10-3	0.438
2.	23.79	Lauroyl peroxide	$C_{24}H_{46}O_4$	105-74-8	0.129
3.	24.3	Pentadecanoic acid	$C_{15}H_{30}O_2$	1002-84-2	0.029
4.	26.6	Cholesta- 22,24 –dien-5-ol, 4,4-dimethyl	$C_{29}H_{48}O$	-	1.621
5.	27.27	7-Methyl-Z-tetradecen-1-ol-acetate	$C_{17}H_{32}O_2$	-	0.59
6.	28.00	Oleic acid	$C_{18}H_{34}O_2$	112-80-1	0.088
7.	28.65	Octadecane,1(ethenyl-oxy)-	$C_{20}H_4O$	930-02-9	0.288
8.	29.88	Octadecane,6-methyl	$C_{19}H_{40}$	10544-96-4	0.637
9.	31.01	Octadecane, 3-ethyl-5-(2-ethylbutyl)-	$C_{26}H_{54}$	55282-12-7	0.78
10.	31.78	**ϒ- Sitosterol**	**$C_{29}H_{50}O$**	**83-47-6**	**30.02**
11.	32.06	**ϒ- Sitosterol**	**$C_{29}H_{50}O$**	**83-47-6**	**31.10**
12.	32.4113	1-Heptatricotanol	$C_{37}H_{76}O$	105794-58-9	0.653
13.	33.09	Octadecane,3-ethyl-5-(2-ethylbutyl)	$C_{26}H_{54}$	55282-12-7	1.550

14.	33.21	Ethyl iso-allocolate	$C_6H_{44}O_5$	-	0.670
15.	33.08	Octadecane, 3-ethyl-5-(2-ethylbutyl)-	$C_{26}H_{54}$	55282-12-7	8.28
16.	34.46	**Lupeol**	**$C_{30}H_{50}O$**	**545-47-1**	**5.92**
17.	35.1557	Stigmasta-3,5-diene-7one	$C_{29}H_{46}O$	2034-72-2	3.42
18.	35.6486	7-Methyl-Z-tetradecen-1-ol-acetate	$C_{17}H_{32}O_2$	-	0.462
19.	36.1482	Ethyl iso-allocolate	$C_6H_{44}O_5$	-	0.28
20.	36.9609	1-Heptatriacotanol	$C_{37}H_{76}O$	105794-58-9	3.34
21.	37.3073	7-Methyl-Z-tetradecen-1-ol-acetate	$C_{17}H_{32}O_2$	-	0.34
22.	37.7935	1-Heptatriacotanol	$C_{37}H_{76}O$	105794-58-9	0.74
23.	38.3131	Ethyl iso-allocolate	$C_6H_{44}O_5$	-	0.58
24.	39.18	Ethyl iso-allocolate	$C_6H_{44}O_5$	-	0.36
25.	39.68	Ethyl iso-allocolate	$C_6H_{44}O_5$	-	0.32
26.	40.37	**Friedelan-3-one**	**$C_{30}H_{50}O$**	**559-74-0**	**7.47%**

The GC-MS results showed that the primary phytoconstituent of **PFF4** is **ϒ- Sitosterol (61.12%). PFF4** showed the presence of 15 different compounds. The major compounds (by % peak area) present in PFF4 are **ϒ- Sitosterol (61.12%), Lupeol (5.92%) and Friedelan-3-one (7.47%)** which constitute 74.51% of total area.

- **ϒ-Sitosterol** is a plant sterol that has been studied for its potential anti-cancer properties[30].
- **Friedelan-3-one** is a triterpenoid compound that has also been studied for its potential anti-cancer properties[31].
- **Lupeol**[32] is a triterpenoid that has been studied for its potential anti-cancer effects against lung cancer.

From literature study it was found that, other compounds present in PFF4 fraction like Lauroyl peroxide, Pentadecanoic acid, 1-Heptatriacotanol, Cholesta-22,24-dien-5-ol, 4,4-dimethyl, Ethyl iso-allocolate,Stigmasta-3,5-diene-7one,Octadecane3-ethyl-5-(2-ethylbutyl),7-Methyl-Z tetradecen-1-ol-acetate, Octadecane,1(ethenyl oxy) and Octadecane,6-methyl were not found to be typically associated with anti-cancer activity, not reported yet in literature.

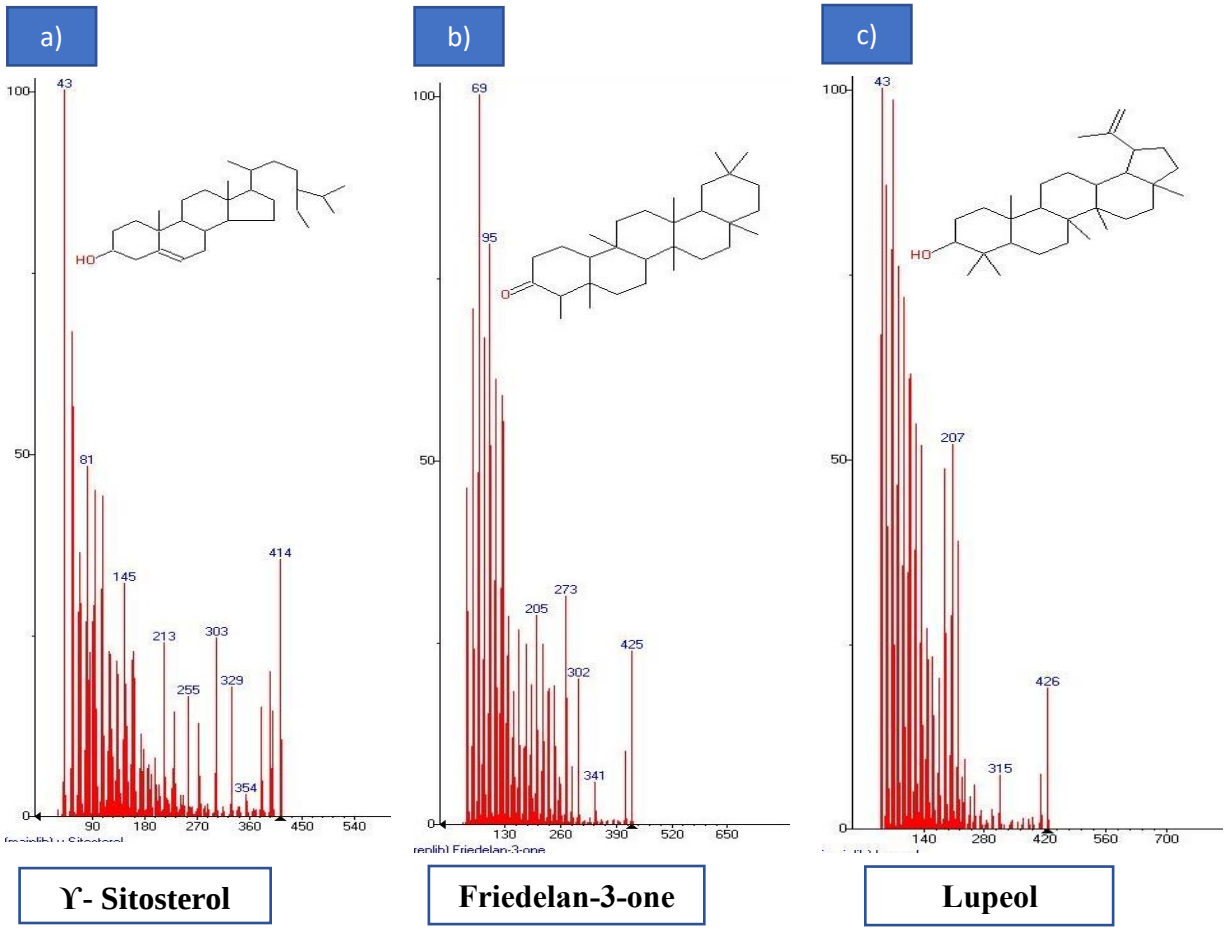

Figure 4.21 Product ion spectrum stating the structure of the major phytocomponents (by %) identified in PFF4 by GC/MS and NIST Library in [A] ϒ- Sitosterol [B] Friedelan-3-one [C] Lupeol.

So, from results of this study and in conjunction with reports on ϒ- Sitosterol, Friedelan-3-one & Lupeol of PFF4 might be responsible for the cytotoxic effect on H460 cells (based upon anticancer activity of these compounds reported in literature).

4.5.2.2.3.3 Nuclear Magnetic Resonance (NMR) Spectroscopy

a) NMR Spectroscopy of PFF3

The NMR Spectrum of PFF3 showed the presence of mixture of compounds rather than a single compound. The NMR spectrum shows multiple peaks at different chemical shifts, which is indicative of the presence of multiple functional groups and/or chemical environments. The presence of multiple compounds can also be inferred from the GC-MS analysis in PFF3 (as explained above). The NMR spectrum of the PFF3 was recorded using a 400 MHz NMR spectrometer with DMSO-d6 as the solvent as shown in Figure 4.22 (a) and (b). The spectrum could potentially include signals from the fatty acids and coumarin derivative. The spectrum showed multiple peaks, including a singlet at 0.88 ppm (CH3 group of palmitic acid)[33], a doublet at 1.60 ppm (CH2 group of palmitic acid), a triplet at 2.06 ppm (CH2 group of linoleic acid), a singlet at 2.42 ppm (CH3 group of alloisoimperatorin), a doublet at 5.30 ppm (olefinic proton of linoleic acid), and a triplet at 6.96 ppm (H-6 of alloisoimperatorin).

Peaks in the region around 0.8-1.5 ppm: These signals are expected to correspond to protons in aliphatic chains, such as those present in fatty acids like dodecanoic acid, tetradecanoic acid, pentadecanoic acid, and n-hexadecanoic acid.

Peaks in the region around 1.5-2.5 ppm: Protons adjacent to carbonyl groups, such as those present in esters, ketones, and carboxylic acids, are typically observed in this region. Compounds identified by GC-MS with carbonyl groups include cyclodecasiloxane, tetradecanoic acid, and pentadecanoic acid.

Peaks in the region around 2.5-3.5 ppm: Protons adjacent to carbon-carbon double bonds are typically observed in this region. Compounds identified by GC-MS with double bonds include 9,12,15-octadecatrienoic acid and Z-7-hexadecenoic acid.

Peaks in the region around 3.5-4.5 ppm: Protons on methylene groups adjacent to carbonyl groups, such as those present in esters and ketones, are typically observed in this region. Compounds identified by GC-MS with ester groups include 9-octadeconoic acid (Z)-2-hydroxy-1-(hydroxymethyl)ethyl ester.

Peaks in the region above 6 ppm: Protons on aromatic rings, such as those present in 1,1-2,2-bis[2,3-dimethylbenzoquinonyl].

a)

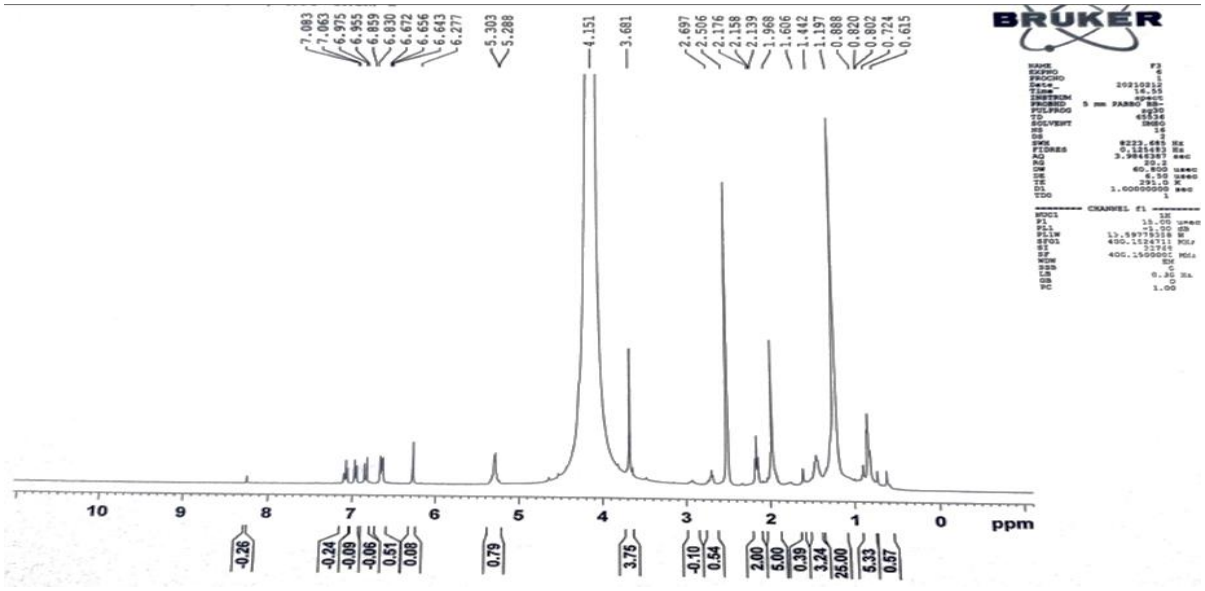

b)

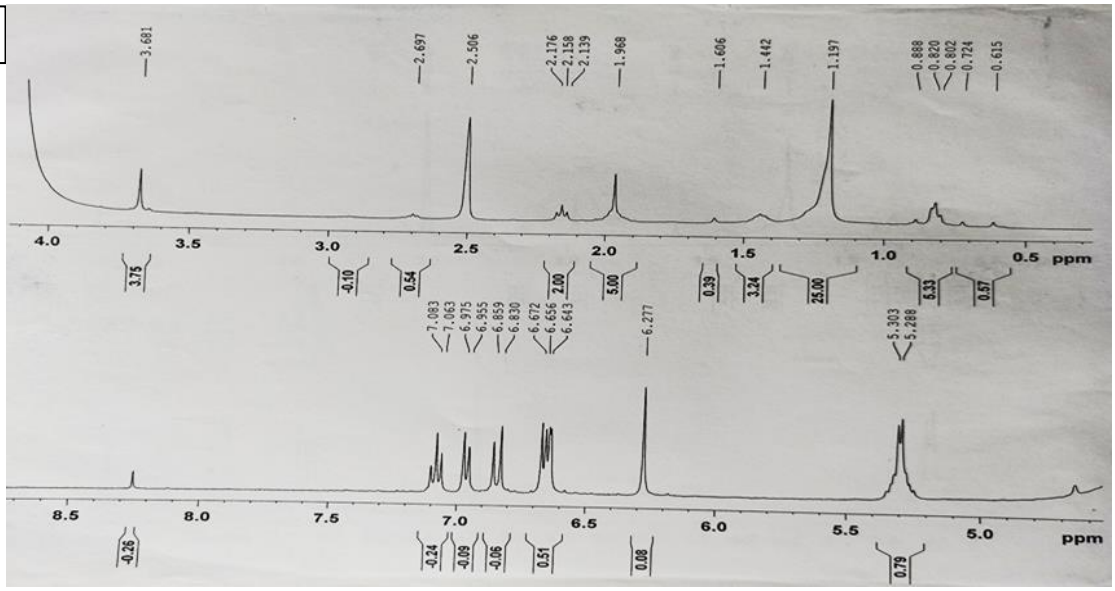

Figure 4.22 a) 1H-NMR spectrum of PFF3. b) Enlarged regions of 1H NMR Spectra of PFF3.

b) NMR Spectroscopy of PFF4

The proton NMR spectrum of the PFF4 dissolved in DMSO-D6 showed multiple distinct peaks, consistent with a mixture of compounds as shown in Figure 4.23 (a) & (b). Tentative assignments of the peaks to gamma-sitosterol, friedalone-one, and heptatriacontanol (maximum present by GCMS) were made based on comparison to known spectra and the reported composition of the sample. The peaks were observed at the following chemical shifts:

0.8-1.0 ppm (broad, -CH2- in heptatriacontanol), 1.2 ppm (cyclohexane protons in gamma-sitosterol), 1.968 ppm (methyl groups in the side chain of friedalone-one), 2.505 ppm (methylene groups in the side chain of friedalone-one), 3.3-3.6 ppm (-CH2OH in gamma-sitosterol), 5.286 ppm (an olefinic (C=C) proton), 6.275 ppm (an aromatic proton), 6.639-6.669 ppm (due to protons on an aromatic ring that is substituted with an electron-withdrawing group, such as a nitro (-NO2) or carbonyl (C=O) group), 6.858 ppm (a proton on an aromatic ring that is substituted with an electron-donating group, such as a methoxy (-OCH3) or amino (-NH2) group), 6.955 ppm (due to a proton on an aromatic ring that is substituted with an electron-donating group, such as a methoxy (-OCH3) or amino (-NH2) group), and 7.061-7.081 ppm (to protons on an aromatic ring).

a)

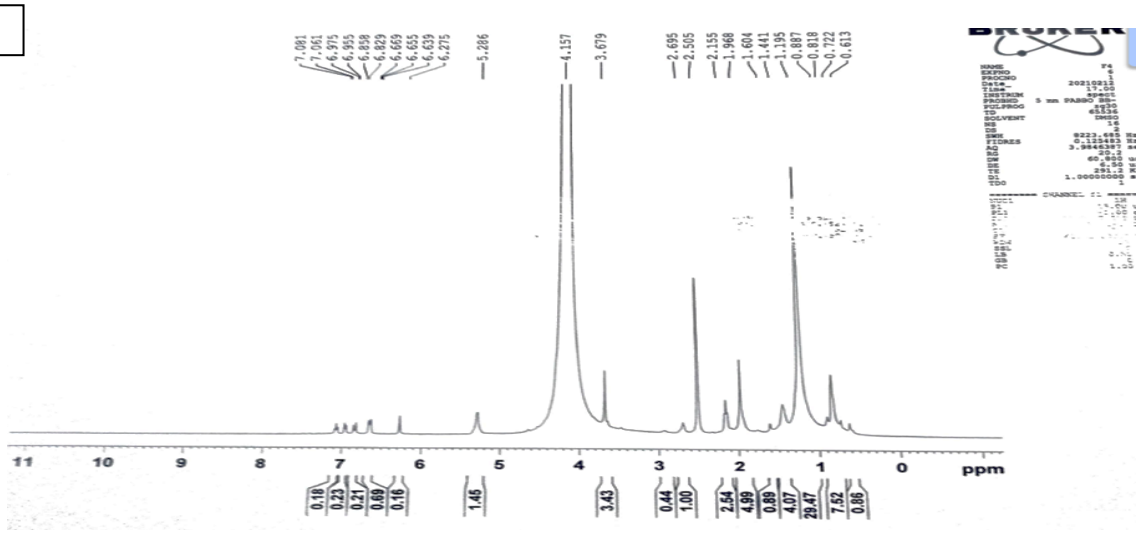

b)

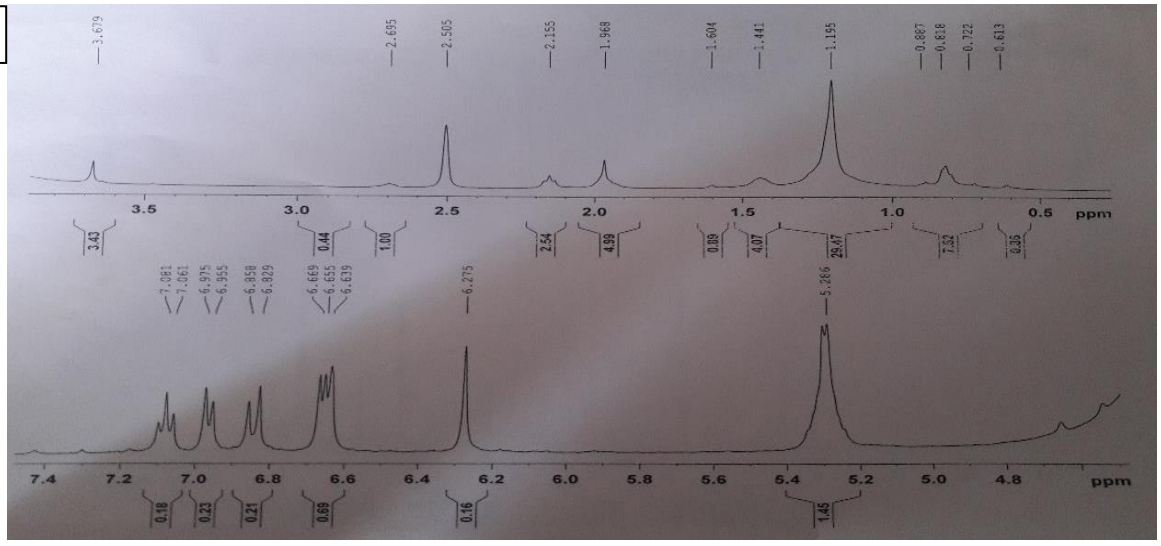

Figure 4.23 a) 1H-NMR spectrum of PFF4 of CBE of *Bauhinia variegata*. b) Enlarged regions of 1H NMR Spectra of PFF4.

4.5.3.2.7 High performance liquid chromatography (HPLC) Analysis

a) HPLC- analysis of PFF3

The RP- HPLC technique was used to identify the compounds present in PFF3. HPLC-DAD chromatogram of PFF3 is shown in Figure 4.24 (a). It is tried to compare with the chromatogram of the phenolic standards[34] in the same HPLC conditions, from the available literature (as not being able to use standards for the comparison), shown figure 4.24 (b).The comparison showed that the PFF3 probably contains Coumarins (3.26 min) at 280nm. From GC-MS data, we found Alloisoimperatorin, 4-(1,1-dimethylallyl]-9 methoxy-7H-furo[3,2-g] [1] benzopyran-7-one (Benahorin) and 10,11-dihydro-2,3,6-trimethoxydibenz(b,f)oxepin-10-one (furocoumarins or psoralens) are Coumarins (in maximum %) present in the PFF3.

a)

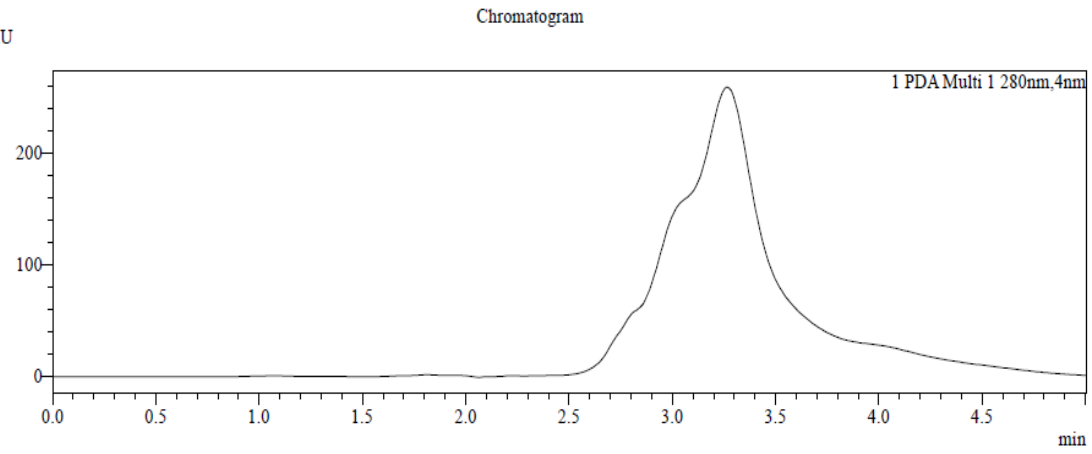

b)

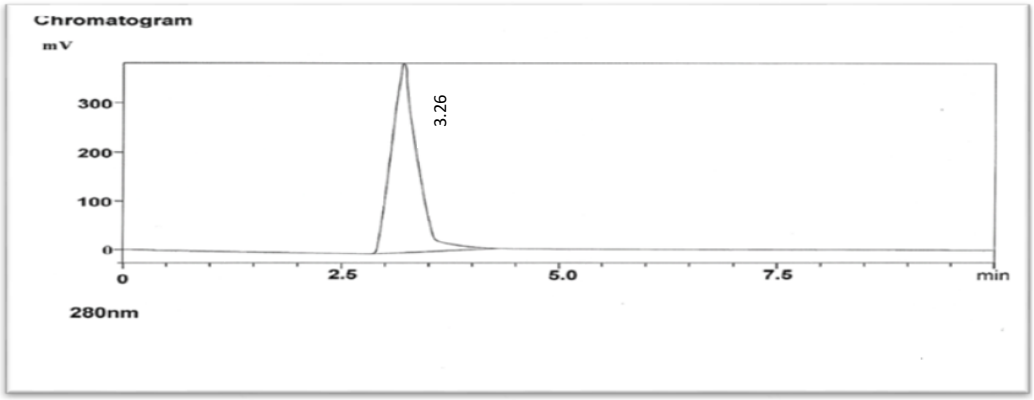

Standard HPLC-DAD chromatogram peak of Coumarin at 280 nm

Figure 4.24 a) Chromatogram peak of PFF3 at 280nm. b) Standard HPLC-DAD chromatogram peak at 280nm.

b) HPLC- analysis of PFF4

The RP- HPLC technique was used to identify the compounds present in PFF4. HPLC-DAD chromatogram of PFF4 is shown in Figure 4.25 (a). Many organic compounds absorb strongly at 280 nm due to the presence of conjugated pi-electron systems, such as those found in aromatic rings and double bonds. It is possible that the peak at 1.881 min in the HPLC-PDA analysis is showing maximum absorption because one or more of the compounds present in the fraction has strong UV absorption at 280 nm. It is also possible that other compounds in the mixture have weaker or no absorption at this wavelength, which could result in a lower or no response from the detector. Compounds that could show maximum absorption at 280 nm and correspond to the peak at 1.881 min in the HPLC-PDA analysis are- Pentadecanoic acid, Gamma-sitosterol and at peak 2.741 min are triterpenoids (comparison from literature reports and in same HPLC conditions). These compounds contain structural features, such as conjugated double bonds and aromatic rings, that can absorb strongly at 280 nm.

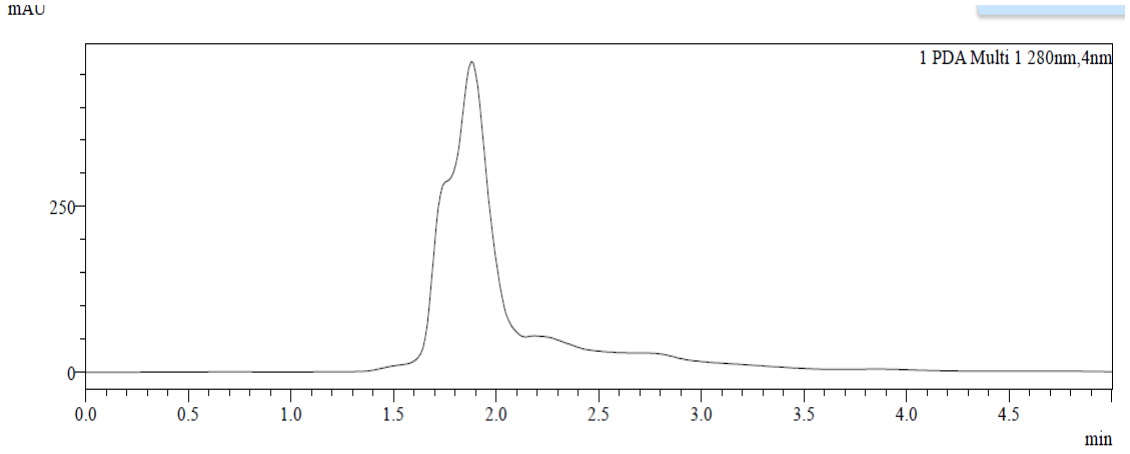

Figure 4.25 a) Chromatogram peak of PFF4 at 280nm.

Section II b) Combination Effect of PFF3 and PFF4 with Paclitaxel in H460 cells

4.6 Introduction

Combination therapy is an emerging strategy in cancer treatment that aims to use multiple drugs with complementary mechanisms of action to achieve efficacy over monotherapy[35]. This is truer when the therapy is plant based. Fractionated plant extracts containing a mixture of

bioactive compounds have shown potential as complementary agents for cancer treatment[36]. PFF3 and PPF4 contains various phytochemicals (as discussed above) such as coumarins, triterpenes, sterols, flavonoids, fatty acids and phenolics that have been shown to possess anti-cancer properties.

The use of fractionated plant extracts in combination with known chemotherapeutic agents represents a promising approach to targeted cancer therapy. These extracts have been reported to exhibit synergistic or additive effects when combined with standard chemotherapy agents, leading to increased cytotoxicity against cancer cells. **Additionally, fractionated plant extracts may also reduce the toxicity and side effects associated with high doses of chemotherapy drugs**[36]. Overall, the combination of fractionated plant extracts with known chemotherapy agents has the potential to enhance the therapeutic efficacy of cancer treatment and improve patient outcomes. It is with this objective that studies on combination of PFF3 and PPF4 were undertaken.

4.6.1 Materials and methods

4.6.1.1 Combination effect of PXT, Gem, PFF3 and PFF4 on cell viability

H460 cells were plated in 96-well plate, at a density of 1x 10^4 cells/well for *in vitro* cytotoxic study by MTT assay and allowed to incubate overnight in CO2 incubator. The cells were treated with medium containing various concentrations of PXT[37] (1.75nM, 3.5nM, 5.5nM, 7.5nM) with a different combinations of PFF3 (25ug/ml, 50ug/ml,100ug/ml) and PFF4 (25ug/ml, 50ug/ml,100ug/ml) as compared to single agents for 24h against H460cells (concentrations based on IC50 as explained above). By using the computer programme CompuSyn software (version 1.0; Paramus, NJ, USA) created by Chou and Martin[38], it was feasible to determine the CI (Combination Index) and DRI (Dose reduction Index) after combination of PTX with PPF3 and PTX with PPF4 respectively. The three types of drug interactions where CI< 1; denoted synergy, CI = 1; additive effect, and CI > 1, antagonism respectively.

4.6.2 Results and Discussion

4.6.2.1 Effect of Combination (PTX & PFF3) on Cell proliferation

To evaluate the combination's capacity to limit cell proliferation, inhibition capacity of the combination of PXT and PFF3 was determined using the MTT assay. Both monotherapy and combination therapy inhibited H460 cell growth in a dose-dependent manner. In monotherapy the IC50 of Paclitaxel and PPF3 was 5.5nM (Figure 4.25a) and 120ug/ml (as explained above

in 4.5.2.2) respectively. The combination dosages was defined referring to the IC50 of both the compounds. When PTX (1.75nM, 3.5nM, 5.5nM) was combined with PFF3 (25ug/ml,50ug/ml,100ug/ml), the IC50 of combination was significantly lower than that of PTX and PFF3 alone at 24hrs. The combination treatment increases the inhibition rate of cell growth as compared to either PTX or PFF3 treatment alone on H460 cells at 24hrs (Figure 4.25b).

The Fraction - affected (Fa) values was calculated to be between 0.353 and 0.547 and CI values were between 0.85 to 0.89 when combination of 1.75nM, 3.5nM,5.5nM PTX with 25ug/ml PPF3 were used. The Fraction - affected (Fa) values were between 0.536 and 0.592 and CI values were between 0.470 to 0.820 when combination of 1.75nM, 3.5nM,5.5nM PTX with 50ug/ml PPF3 were used. The Fraction - affected (Fa) values were between 0.515 and 0.604 and CI values were between 0.759 to 0.913 when combination of 1.75nM, 3.5nM,5.5nM PTX with 100ug/ml PPF3 were used. These results showed significant synergistic effects (<1) between PTX & PFF3 at different concentrations. **The highest synergistic effect was observed with a combination of PTX 1.75nM & PFF3-50ug/ml (CI= 0.47).** Thus, PPF3 can be effective to combat H460 cells, and its efficacy can be enhanced through synergistic effects with Paclitaxel (PTX). The mean DRI of PXT and PPF3 in the combination therapy was 3.8 and 4.8; which means three and four-fold dose reduction compared to monotherapy. The CI values and plot of combination is shown in Figure 4.45 b, c. CI range; 0.1-0.3 - strong synergism, 0.3-0.7 – synergism, 0.7-0.85- moderate synergism, 0.85-0.90 – slight synergism, 0.9-1.10 – nearly additive, >1 antagonism.

a

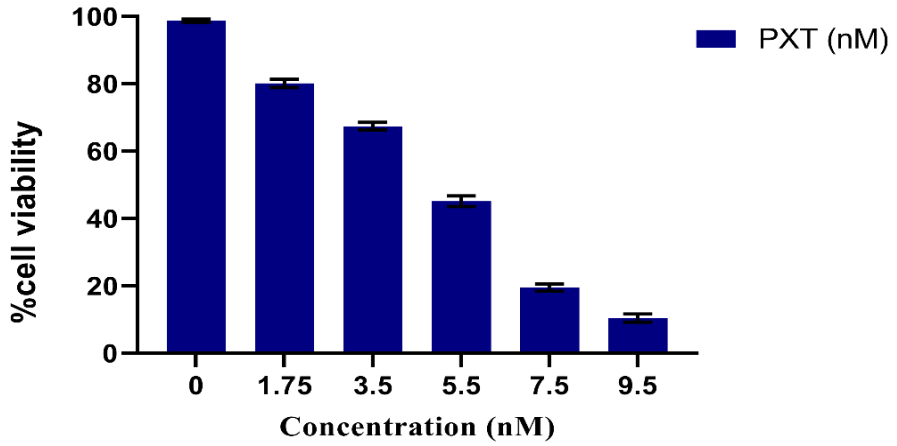

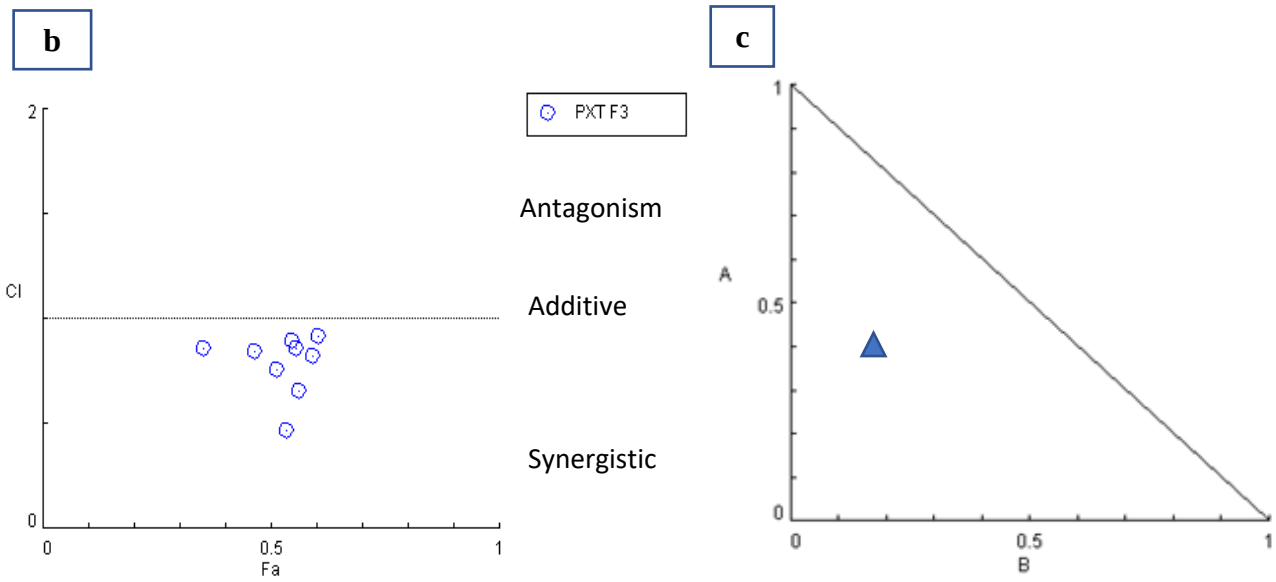

Figure 4.26 a) Cell growth inhibitory effect of Paclitaxel (PXT) as monotherapy on H460 cells. b) Combination Index (CI) and of Paclitaxel (PXT) and PFF3 in H460 cells was calculated by CompuSyn software, c) Normalized Isobologram for Combo; CI < 1 and CI > 1 indicate synergistic and antagonistic effects. Fa: fraction affected; CI: Combination index. Fa of 0.5 represents 50% inhibition.

4.6.2.2 Effect of Combination (PTX & PFF4) on Cell proliferation

To evaluate the combination's capacity to limit cell proliferation, inhibition capacity of the combination of PXT and PFF4 was determined using the MTT assay. In monotherapy, the IC50 of Paclitaxel and PPF3 was 5.5nM (Figure 4.26a) and 130ug/ml (as explained above in section 4.5.2.2) respectively. The combination dosages were defined referring to the IC50's of both the compounds. When PTX (1.75nM, 3.5nM, 5.5nM) was combined with PFF4 (25ug/ml,50ug/ml,100ug/ml), there was no significant synergism observed between PTX and PPF4 at 24hrs (Figure 4.27). The mean CI value of combination against H460 was >1 means antagonistic behaviour. So, working with PFF4 alone would be a better anti-cancer agent than in combination with PXT.

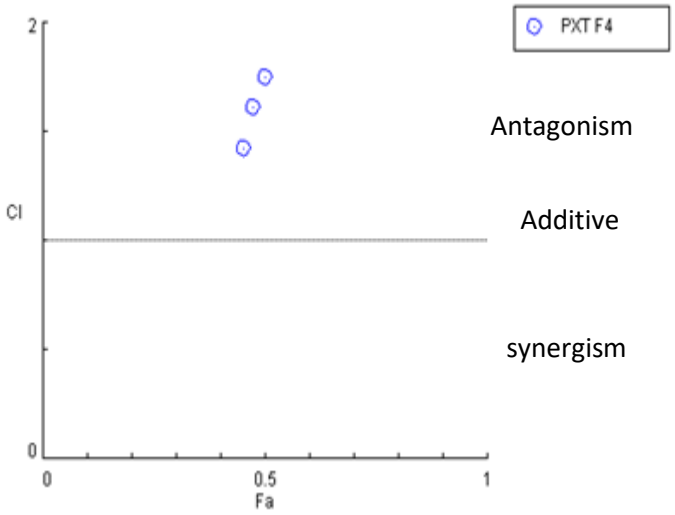

Figure 4.27 Combination Index values and plot (Fa-CI plot) of interaction between Paclitaxel and PPF4 in H460 cells plotted by CompuSyn software. Fa: fraction affected; CI: Combination index. Fa of 0.5 represents 50% inhibition.

4.6.3 Conclusion

In the present study, isolation & identification of phytocomponents from PEBE and CBE of *Bauhinia variegata* was done by analytical methods and its effects was checked on cytotoxic parameters in lung cancer cell lines respectively. The extract was first fractionated using column chromatography, subjected to TLC. The partially purified compounds were collected. Based upon characterization by GCMS, followed by identification by NIST library, and from percentages of compounds present in the PEBE and taking note of reports, cytotoxic effect of oleic acid, palmitic acid and heptadecanoic acid was checked on A549 cells. Oleic acid was found to be most cytotoxic on A549 cells at 48 h treatment and was used for the further study to check the biochemical mechanism involved in causing cell death in A549 cells. The cytotoxic effect of purified fractions of CBE on H460 cell line was also done by MTT assay and identification of phytocomponents by analytical methods was also carried out. PFF3 and PFF4 showed most cytotoxic effect at 24hrs on H460 cells among all other fractions. PFF3 and PFF4 were more potent after 24 h treatment; hence this time point was selected for further experiments. Characterization of PFF3 and PFF4 of CBE was done by FTIR, GCMS, NMR and HPLC. Different analytical methods revealed the presence of mixture of compounds in the PFF3 & PFF4 of CBE of *Bauhinia variegata*. PPF3 fraction showed highest proportion of different fatty acids and Coumarin derivates while PPF4 showed the highest proportion of ϒ-Sitosterol and different triterpenoids which have been shown to possess anti-cancer properties in various *in vitro* and *in vivo* studies.

In order to lower the dosage of Paclitaxel (PTX), currently being used for the treatment, the synergistic effects of PTX and PPF3 was also investigated in this study. Combining PTX and PPF3 might reduce PTX's adverse effects rather than its cytotoxic effects while maintaining its ability to kill H460 cells. The current study shows that PTX and PPF3 had a synergistic impact on H460 cells *in vitro*, and that an increase in the level of induced apoptosis may be the cause of the potentiation of the cytotoxicity against the H460 cells. As a result, the mixture of PTX and PPF3 has the potential to be employed as a chemotherapeutic agent to treat lung cancer while lowering the toxicity of the dose of PTX that is currently being used.

4.6.4 References

1. Pandey MM, Rastogi S, Rawat AKS. Indian traditional ayurvedic system of medicine and nutritional supplementation. *Evidence-based Complement Altern Med*. 2013;2013. doi:10.1155/2013/376327
2. Shi Y, Zhang C, Li X. Traditional medicine in India. *J Tradit Chinese Med Sci*. 2021;8:S51-S55. doi:10.1016/j.jtcms.2020.06.007
3. Mukherjee PK, Harwansh RK, Bahadur S, et al. Development of Ayurveda – Tradition to trend. *J Ethnopharmacol*. 2017;197:10-24. doi:10.1016/j.jep.2016.09.024
4. Altemimi A, Lakhssassi N, Baharlouei A, Watson DG, Lightfoot DA. Phytochemicals: Extraction, isolation, and identification of bioactive compounds from plant extracts. *Plants*. 2017;6(4). doi:10.3390/plants6040042
5. Tungmunnithum D, Thongboonyou A, Pholboon A, Yangsabai A. Flavonoids and Other Phenolic Compounds from Medicinal Plants for Pharmaceutical and Medical Aspects: An Overview. *Medicines*. 2018;5(3):93. doi:10.3390/medicines5030093
6. Chiocchio I, Mandrone M, Tomasi P, Marincich L, Poli F. Plant secondary metabolites: An opportunity for circular economy. *Molecules*. 2021;26(2). doi:10.3390/molecules26020495
7. Erecta T, Devika LR, Koilpillai J. Column Chromatographic Separation of Bioactive Compounds From. *Int J Pharm Sci Res*. 2015;6(2):762-766. doi:10.13040/IJPSR.0975-8232.6(2).762-66
8. A NVK, P PK, Mahendran B, B VR. Column Chromatography Purified Phytochemicals Identified in Phr agmyt es val l at or i a Leaf Ethanolic Extract. *Amer ican J Adv Drug Deliv*. Published online 2013:611-627.
9. Rashid R., Wani MH., Hajam GN., Hussain A. Extraction Method and Isolation of

Phytoconstituents from the Chloroform Extract of Plant Solanum Nigrum L . By Colunm Chromatography. *Int J Adv Res Ideas Innov Technol ISSN*. 2017;3(6):4-8.

10. Aiswarya G, Gupta R, Kambhoja S. Isolation of 28-pentyl-3-galloyl-betulinate and11-hydroxy friedelane from the plant Argyreia speciosa. *Res J Pharm Biol Chem Sci*. 2010;1(3):207-221.
11. Gini TG, Jeya Jothi G. Column chromatography and HPLC analysis of phenolic compounds in the fractions of Salvinia molesta mitchell . *Egypt J Basic Appl Sci*. 2018;5(3):197-203. doi:10.1016/j.ejbas.2018.05.010
12. Pakkirisamy M, Kalakandan SK, Ravichandran K. Phytochemical screening, GC-MS, FT-IR analysis of methanolic extract of Curcuma caesia roxb (black turmeric). *Pharmacogn J*. 2014;9(6):952-956. doi:10.5530/pj.2017.6.149
13. Jiang L, Wang W, He Q, et al. Oleic acid induces apoptosis and autophagy in the treatment of Tongue Squamous cell carcinomas. *Sci Rep*. 2017;7(1):1-11. doi:10.1038/s41598-017-11842-5
14. Giulitti F, Petrungaro S, Mandatori S, et al. Anti-tumor Effect of Oleic Acid in Hepatocellular Carcinoma Cell Lines via Autophagy Reduction. *Front Cell Dev Biol*. 2021;9(February):1-16. doi:10.3389/fcell.2021.629182
15. Yu X, Peng W, Wang Y, et al. Palmitic Acid Inhibits the Growth and Metastasis of Gastric Cancer by Blocking the STAT3 Signaling Pathway. *Cancers (Basel)*. 2023;15(2):388. doi:10.3390/cancers15020388
16. Xu C, Wu P, Gao J, et al. Heptadecanoic acid inhibits cell proliferation in PC-9 non-small-cell lung cancer cells with acquired gefitinib resistance. *Oncol Rep*. 2019;41(6):3499-3507. doi:10.3892/or.2019.7130
17. Li S, Zhou T, Li C, et al. High metastaticgastric and breast cancer cells consume oleic acid in an AMPK dependent manner. *PLoS One*. 2014;9(5). doi:10.1371/journal.pone.0097330
18. Zafaryab M, Fakhri KU, Khan MA, Hajela K, Rizvi MM. In vitro assessment of cytotoxic and apoptotic potential of palmitic acid for breast cancer treatment. *Int J Life Sci Res*. 2019;7(1):166-174. www.researchpublish.com
19. Menendez JA, Vellon L, Colomer R, Lupu R. Oleic acid, the main monounsaturated fatty acid of olive oil, suppresses Her-2/neu (erb B-2) expression and synergistically enhances the growth inhibitory effects of trastuzumab (Herceptin^{TM}) in breast cancer cells with Her-2/neu oncogene amplification. *Ann Oncol*. 2005;16(3):359-371. doi:10.1093/annonc/mdi090

20. Wang X. Dietary palmitic acid promotes tumor growth and epithelial-mesenchymal transformation in prostate cancer. Published online 2021.
21. Zhang X, Li X, Xiong G, et al. Palmitic Acid Promotes Lung Metastasis of Melanomas via the TLR4/TRIF-Peli1-pNF-κB Pathway. *Metabolites*. 2022;12(11):1132. doi:10.3390/metabo12111132
22. Zhang H, Zheng Y, Han D, et al. Combination of Palmitic Acid and Methylseleninic Acid Induces Mitochondria-Dependent Apoptosis via Attenuation of the IRE1α Arm and Enhancement of CHOP in Hepatoma. *ACS Omega*. 2021;6(24):15708-15715. doi:10.1021/acsomega.1c00959
23. Bharath B, Perinbam K, Devanesan S. Evaluation of the anticancer potential of Hexadecanoic acid from brown algae Turbinaria ornata on HT – 29 colon cancer cells. *J Mol Struct*. 2021;1235:130229. doi:10.1016/j.molstruc.2021.130229
24. Nishioka N, Matsuoka T, Yashiro M, Hirakawa K, Olden K, Roberts JD. Linoleic acid enhances angiogenesis through suppression of angiostatin induced by plasminogen activator inhibitor 1. *Br J Cancer*. 2011;105(11):1750-1758. doi:10.1038/bjc.2011.434
25. Lu X, Yu H, Ma Q, Shen S, Das UN. Linoleic acid suppresses colorectal cancer cell growth by inducing oxidant stress and mitochondrial dysfunction. *Lipids Health Dis*. 2010;9:10-13. doi:10.1186/1476-511X-9-106
26. Pilkington GJ, Parker K, Murray SA. Approaches to mitochondrially mediated cancer therapy. *Semin Cancer Biol*. 2008;18(3):226-235. doi:10.1016/j.semcancer.2007.12.006
27. Jóźwiak M, Filipowska A, Fiorino F, Struga M. Anticancer activities of fatty acids and their heterocyclic derivatives. *Eur J Pharmacol*. 2020;871:172937. doi:10.1016/j.ejphar.2020.172937
28. Wu Y, Xu J, Liu Y, Zeng Y, Wu G. A Review on Anti-Tumor Mechanisms of Coumarins. *Front Oncol*. 2020;10(December):1-11. doi:10.3389/fonc.2020.592853
29. Derivatives I--yl, Raffa D, Daidone G, Maggio B, Schillaci D, Plescia F. Synthesis and Antiproliferative Activity of Novel. 1999;4:317-320.
30. Sundarraj S, Thangam R, Sreevani V, et al. γ-Sitosterol from Acacia nilotica L. induces G2/M cell cycle arrest and apoptosis through c-Myc suppression in MCF-7 and A549 cells. *J Ethnopharmacol*. 2012;141(3):803-809. doi:10.1016/j.jep.2012.03.014
31. Aguilar MG, Sousa GF, Evangelista FCG, Sabino AP, Vieira Filho SA, Duarte LP. Imines and lactones derived from friedelanes and their cytotoxic activity. *Nat Prod Res*. 2020;34(6):810-815. doi:10.1080/14786419.2018.1508137
32. Babu ST. Study on the Anti Metastatic and Anticancer Activity of Triterpene Compound

Lupeol in Human Lung Cancer. *Int J Pharm Sci Res*. 2019;4(2):763-773. doi:10.13040/IJPSR.0975-8232.10(2).721-27

33. Di Pietro ME, Mannu A, Mele A. NMR determination of free fatty acids in vegetable oils. *Processes*. 2020;8(4). doi:10.3390/PR8040410
34. Ali OT, Mohammed MJ. Bioactive phenolic compounds from natural zygophyllum fabago plant: Isolation, purification and characterization. *J Glob Pharma Technol*. 2019;11(7):794-800.
35. Pezzani R, Salehi B, Vitalini S, et al. Synergistic effects of plant derivatives and conventional chemotherapeutic agents: An update on the cancer perspective. *Med*. 2019;55(4):1-16. doi:10.3390/medicina55040110
36. Lim CP, Yam MF, Asmawi MZ, et al. Cytostatic and antiproliferative activities of f5 fraction of crinum amabile leaf chloroform extract showed its potential as cancer chemotherapeutic agent. *Evidence-based Complement Altern Med*. 2019;2019. doi:10.1155/2019/7521504
37. Tan KT, Li S, Li YR, Cheng SL, Lin SH, Tung YT. Synergistic Anticancer Effect of a Combination of Paclitaxel and 5-Demethylnobiletin Against Lung Cancer Cell Line In Vitro and In Vivo. *Appl Biochem Biotechnol*. 2019;187(4):1328-1343. doi:10.1007/s12010-018-2869-1
38. Cells C, Kamran S, Sinniah A, Chik Z. Diosmetin Exerts Synergistic Effects in Combination with. Published online 2022.